

**AN INVESTIGATION OF SOLID-LIQUID FLOW
DISTRIBUTION THROUGH SLURRY PIPELINE**

**A
THESIS**

Submitted in partial fulfillment of the requirements for the award of degree of

Master of Engineering (M.E.)

**In
Thermal Engineering**

**Submitted by
KUSHAL PURI
(ROLL NO. 801283015)**



Under the guidance of

**Dr. S.K. MOHAPATRA
(Senior Professor, DOAA)**

**DEPARTMENT OF MECHANICAL ENGINEERING
THAPAR UNIVERSITY, PATIALA – 147004**

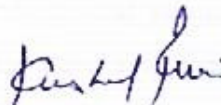
JULY 2014

DECLARATION

I hereby declare that this thesis report entitled "An Investigation of Solid-Liquid Flow Distribution Through Slurry Pipeline" submitted in the partial fulfillment of the requirements for the award of degree of Master of Engineering in Thermal Engineering, in the Mechanical Department, Thapar University, Patiala, is wholly my own work. This matter embodied in this report has not been submitted in part or full to any other university or institute for the award of any degree.

Date:


Place:



Kushal Puri

(801283015)

This is to certify that above statement made by the student concerned is correct and true to the best of my knowledge & belief.

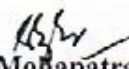


Dr. S.K. Mohapatra
Senior Professor, DOAA
Thapar University, Patiala

Countersigned by



Dr. Ajay Batish
Professor & Head of Department
Thapar University, Patiala



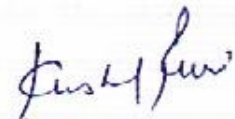
Dr. S.K. Mohapatra
Dean Academic Affairs
Thapar University, Patiala

ACKNOWLEDGEMENT

First of all, I would like to express my gratitude to **Dr. S.K. Mohapatra**, Senior Professor, Mechanical Engineering Department and Dean Academic Affairs, Thapar University, Patiala for his patience guidance and support throughout this report. I am truly very fortunate to have the opportunity to work with him. I found his guidance to be extremely valuable.

I also express my special thanks to **Dr. Ajay Batish**, Professor and Head, Mechanical Engineering Department, **Dr. S.K Mohapatra**, Sr. Professor, Mechanical Engineering Department, and Dean Academic Affair, Thapar University Patiala and P.G. coordinator **Mr. Satish Kumar**, Assistant Professor providing me opportunity to conduct this work and bring it out in present form.

Last but not the least; I want to convey my heartiest gratitude to my parents and my friends for their immeasurable love, support and encouragement.



Kushal Puri

ABSTRACT

Pipeline transport is considered environment friendly and economical as compared to rail and road transport. To design the pipelines and its associated facilities designers need accurate information regarding pressure drop, critical velocity, flow regimes, hold up etc. Many large slurry pipelines were built and operating around the world. Such flows are complex and the correlations presently available in open literatures for the above mentioned parameters have a prediction error 25-35 %. This much of error in design and slurry operation has serious cost implication and is totally unacceptable.

In the present study, an attempt has been made to simulate the mineral (zinc taling and lime water) slurry flow through straight pipeline to predict the pressure drop, velocity profile and behavior of solid particles. To simulate the slurry flow commercial CFD software FLUENT 14.5 has been used. An Eulerian model based on kinetic theory of granular flow is used to represent multiphase phenomenon. To describe the turbulence present in the flow Standard $k-\epsilon$ turbulent model coupled with standard wall treatment with dispersed properties has been used. All these models are part of CFD software package FLUENT 14.5. The Simulation is performed on pipeline having 42 mm diameter and 7 m length. The experimental data consist of zinc water slurry and lime water slurry with 33 μm particle diameter. The velocity of the flow is varied from 1.5 to 3.5 m/s and concentration is varied from 30 to 60 % by weight. The effect of increase in particle diameter at same concentration is also analyzed and comparison is made on pressure drop, power consumed, and volume fraction contour. Before performing simulation on the desired slurry, first the simulation results are validated with the experimental data taken from the open literature. The simulated results indicate that the particles are asymmetrically distributed in the vertical plane with the degree of asymmetry increases with increase in particle diameter. The predicted pressure drop at different velocities and concentration shows good agreement with experimental data obtained from open literature.

CONTENTS

Chapters	Title	Page No.
	<i>DECLARATION</i>	i
	<i>ACKNOWLEDGEMENT</i>	ii
	<i>ABSTRACT</i>	iii
	<i>TABLE OF CONTENT</i>	iv
	<i>LIST OF FIGURES</i>	vi
	<i>LIST OF TABLES</i>	viii
	<i>NOMENCLEATURE</i>	ix
Chapter 1	INTRODUCTION	1-10
1.1	Slurry Transportation System	2
1.2	Types of Fluid	4
1.3	Slurry Flow	5
1.4	Classification of Flow Regimes	6
1.4.1	Classification Based on Particle Size	7
1.4.2	Classification Based on Solid Concentration	8
1.5	Critical Velocity and Hold UP	8
1.6	Pressure Drop	8
1.7	Concentration and Velocity Profile	9
1.8	Motivation of Present Work	9
Chapter 2	LITERATURE REVIEW	11-23
Chapter 3	COMPUTATIONAL FLUID DYNAMICS	24-39
3.1	Various Discretization Schemes	25
3.2	CFD Analysis Steps	26
3.2.1	Pre Processing	27
3.2.1.1	Geometry Creation or Input	27
3.2.1.2	Mesh generation	27
3.2.2	Solver	27
3.2.3	Post Processing	27
3.3	Advantages and Disadvantages of CFD	28
3.4	Applications of CFD	28

3.5	Multiphase Modeling	29
3.5.1	Approaches to Multiphase Modeling	29
3.6	CFD Multiphase Model Formulation	33
3.6.1	Eulerian Model	34
3.7	Selection Criteria for Multiphase Model	36
3.8	Turbulence Modeling	37
3.8.1	Complexity of Turbulence Model	37
3.8.2	Classification of Turbulent Model	38
3.8.3	Guidelines for Selecting RANS Turbulence Model	39
Chapter 4	SIMULATED FLOW DISTRIBUTION IN SLURRY PIPE	40-62
4.1	Modeling and Meshing	40
4.2	Properties of Material	43
4.3	Boundary condition and solution strategy	44
4.4	Validation of CFD Simulation	46
4.5	Result and Discussion	47
4.5.1	Pressure Drop and Power Consumption for Zinc and Lime Slurry	47
4.5.1.1	Zinc Slurry	47
4.5.1.2	Lime Slurry	48
4.5.2	Concentration Profile for Zinc and Lime Slurry	50
4.5.2.1	Concentration Profile for Zinc Slurry	50
4.5.2.2	Concentration Profile for Lime Slurry	53
4.5.3	Velocity Profile	54
4.5.3.1	Velocity Profile for Zinc Slurry	55
4.6	Effect of Particle Size	58
4.6.1	Effect of Particle size on Pressure Drop and Power Consumption	58
4.6.2	Effect of Particle size on Solid Volume Fraction Contour	59
Chapter 5	CONCLUSIONS AND FUTURE SCOPE	63-64
5.1	Conclusions	63
5.2	Future Scope	64
	REFERENCES	65-67

LIST OF FIGURES

Figure No.	Description	Page No.
1.1	Schematic layout of a long distance slurry pipeline	3
1.2	Flow regimes for slurry flow in a horizontal pipeline	7
3.1	Various discretization techniques	25
3.2	CFD Analysis procedure	26
3.3	Different approaches to multiphase modeling	29
3.4	Euler Lagrange approach visualization	30
3.5	Euler Euler approach visualization	31
3.6	Guidelines for choosing multiphase model	37
3.7	Various Turbulence Model	39
4.1	Crosssectional View of Pipe (dia.: 42 mm)	41
4.2	Isometric view of pipe (length 7000 mm)	41
4.3	Pipe mesh with 230000 number of elements	42
4.4	Mesh with 332000 elements	42
4.5	Mesh with 415670 elements	42
4.6	Mesh with 565322 elements	43
4.7	Mesh with 630558 elements	43
4.7	Comparison between measured and predicted pressure drop at various concentration	47
4.8(a)	Pressure drop comparison at different concentration for zinc slurry	48
4.8(b)	Power required at various concentrations and velocities for zinc slurry	49
4.9(a)	Pressure drop comparison at various concentrations for lime slurry	49
4.9(b)	Power required at various concentrations and velocities for lime slurry	50
4.10 (i)	Volume fraction contour at 30% concentration by weight at different velocities	51
4.10 (ii)	Volume fraction contour at 40% concentration by weight at different velocities	52
4.10 (iii)	Volume fraction contour at 50% concentration by weight at different velocities	52
4.10 (iv)	Volume fraction contour at 60% concentration by weight at different velocities	53
4.11 (i)	Volume fraction contour at 30% concentration by weight at different velocities	54
4.11 (ii)	Volume fraction contour at 50% concentration by weight at different velocities	54
4.11 (iii)	Volume fraction contour at 60% concentration by weight at different velocities	55
4.12	Vertical velocity profile at 1 m/s at 60% concentration by weight	56
4.13	Vertical velocity profile at 1.5 m/s at 60% concentration by weight	57
4.14	Vertical velocity profile at 2 m/s at 60% concentration by weight	57
4.15	Vertical velocity profile at 2.5 m/s at 60% concentration by weight	58
4.16	Vertical velocity profile at 3 m/s at 60% concentration by weight	58
4.17	Vertical velocity profile at 3.5 m/s at 60% concentration by weight	59

4.18(a)	Comparison of pressure drop at different velocities at 40% concentration by weight of zinc slurry at two different particle sizes	60
4.18(b)	Power required at 40% concentration at different velocities for zinc slurry at two different particle sizes.	60
4.19	Comparison of solid volume fraction contour at different velocities at 40% concentration by weight of zinc slurry at two different particles size.	63

LIST OF TABLES

Table No.	Description	Page No
1.1	Constitutive equations of non-Newtonian fluids	4
3.1	Selection of Turbulence Model	40
4.1	Grid independence of the simulation result	43
4.2	Rheological properties of zinc water slurry with specific gravity of zinc 2.844	44
4.3	Rheological properties of lime water slurry with specific gravity of lime 2.320	44
4.4	Inputs for simulation in FLUENT	46

NOMENCLEATURE

C_{vi}	In Situ Volumetric Concentration
C_{vd}	Delivered Concentration of Solid
D	Diameter of Pipe
d_p	Particle Diameter
d_{wm}	Weighted mean diameter, (mm)
d_{50}	Median particle diameter, (mm)
e_{ss}	Coefficient of Restitution
$g_{o,ss}$	Distribution Function
K_{sl}	Liquid Solid Exchange Coefficient
P	Power, kW
\vec{u}	Fluid Phase Velocity
u_p	Particle Velocity
v_l	Velocity of liquid Phase
V_s	Velocity of Solid Phase
α_l	Volume Fraction of Liquid Phase
α_s	Volume Fraction of Solid Phase
∇p_s	Collisional Solid Stress
ρ_f	Density of fluid
ρ_s	Density of Solid Material
ρ_m	Density of Mixture
$\bar{\tau}_s$	Phase Stress Tensor for Solid
$\bar{\tau}_l$	Phase Stress Tensor for Fluid
τ	Shear Stress
τ_y	Yield Stress
γ	Shear Strain
λ_s	Bulk Viscosity of Solid
μ	Dynamic Viscosity
μ_s	Shear Viscosity of Solid
$\mu_{s,col}$	Collisional Viscosity

$\mu_{s,kin}$	Kinetic Viscosity
$\mu_{s,fr}$	Frictional Viscosity
η	Apparent Viscosity
θ_s	Granular Temperature
ϕ	Angle of Internal Friction

The hydraulic transport of solid material in a particle form is a well-known method in the chemical and mining industries. In most industrial processes, fluids are used as a medium for material transport. A complete knowledge of the principles that rule the phenomena involving fluids transportation lead to more efficient and secure system. Pipeline transport is an environment friendly and is considered economical way as compared to rail and road transport **Wilson et al. (2005)**. Early studies for slurry transportation through pipeline were based on moderate concentration (25% by volume). Much larger concentrations are now in common use. The flow of highly concentrated multi sized particulate slurry is very complex **Kaushal et al. (2013)**. Designers need precise information regarding hold up, critical velocity, pressure drop, flow regimes etc. to design the pipelines and its associated facilities. However in many industries, such as petroleum, chemical, oil and gas industry, two-phase or multiphase flow is frequently observed. Multiphase flow is defined as the simultaneous flow of several phases, with the simplest case being a two-phase flow. A two-phase mixture consist of two distinct phase such as gas-solid, gas-liquid, or liquid solid that co-exist in arbitrary space. For most particulate two-phase flow (i.e. liquid-solid or gas-solid flows), the fluid phase is continuously connected and the solid phase exist as discrete particles. The study of two-phase flow is vital from the viewpoint of practical applications (pneumatic transport and hydro-transport of particles in pipes) and natural phenomenon (e.g. sediment transport in water bodies, biological/biomedical flow). Flow which include granular materials are found in the chemical, mining, petrochemical and food industry.

The physics of two-phase flow is more complex than for single-phase flow due to presence of dispersed phase. Further complications, which are sometimes difficult to elucidate, arise when the dispersed phase undergoes either a fluctuating or continuous contact motion with other particles and/or when the flow is affected by turbulence. In this case, the solids phase does not follow the flow but interacts and modifies the fluid phase flow feature. Turbulence modulation in two-phase turbulent flows is also of importance for industrial applications.

A few of the reasons for the increasing popularity of the pipeline system are its economy, reliability, low maintenance cost, round the year availability at the user's end. It is also extremely safe and leads to minimum environmental pollution. Further, a pipeline transportation system broadens the economic reach of the mineral deposit that may be utilized. Some more advantages associated with the pipeline transportation of solids are listed below:

- 1) Simplicity of installation as compared with the construction of a new high way or rail road.
- 2) Low man-power requirement for construction, operation and maintenance.
- 3) Possibility of complete automation.
- 4) Elimination of traffic problem associated with trucking.

However, the pipeline transportation system has also some limitations, some of these are:

- 1) The initial capital cost is relatively high.
- 2) The pipeline transportation system is solely dedicated to transportation of solids where as rail road or a highway has multipurpose utility.
- 3) The pipeline transportation system requires water or other liquid as the carrier fluid in large volume which may not be easily available at all the places at all the time.

1.1 Basic Slurry Transportation System

Solids can be transported through pipeline rather hydraulically or pneumatically. The difference between two is only in nature of the fluid used for motion of the solid particles. A slurry transportation system may be different for different materials that can be transported through pipeline, depending on the material and end requirement. However, a general schematic layout of slurry transportation system is shown in fig.1.1. A slurry transportation system can be broadly divided into three sub-systems namely-

- i) Slurry preparation facility
- ii) Main pipeline and pumps
- iii) Terminal facility

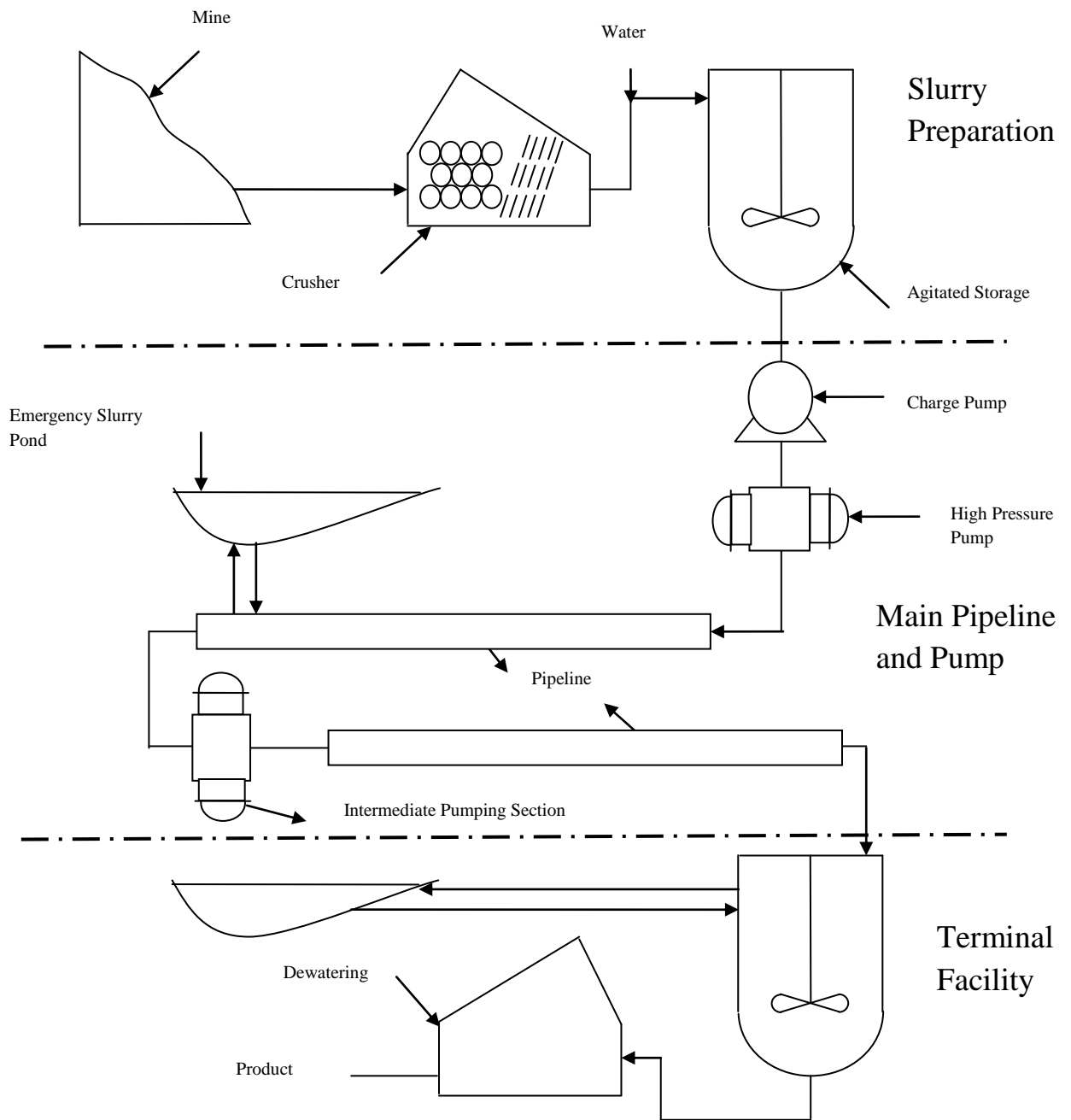


Fig.1.1 Schematic layout of a long distance slurry pipeline **Abulnaga (2002)**.

The first step in the processing cycle is to reduce the solids to convenient size by crushing so that it is technically and economically feasible to provide the necessary power requirement for

their suspension and their transportation by the carrier fluid. Next, the solid is mixed with the carrier liquid and the proportion of solid to the liquid is adjusted to an optimum value. Finally the slurry is stored in agitated /non-agitated storage tank as required.

Depending on the distance over which transportation is to be effected, the total pumping requirement may be provided from either one or more than one point along the length of pipeline. At the terminal end, the slurry is received in storage tank. This slurry then needs to be dewatered, filtered and dried to the extent desired for an end utilization of the solids.

1.2 Types of Fluid

A fluid is substance that continually deforms under an applied shear stress. Viscosity is the resisting property of a fluid to shearing force. It describes fluid's internal resistance to flow and is a material property which relates the shear stress (τ) and the time rate of shear strain ($\dot{\gamma}$) in a moving fluid. Basic equation relating an applied shear stress and time rate of deformation of a fluid represent in equation below.

$$\tau = \eta \dot{\gamma} \tag{1.1}$$

In equation 1.1, η is the apparent viscosity of the fluid. For Newtonian mixtures, the apparent viscosity is equal to the fluid viscosity ($\eta = \mu$), which is independent of both applied shear stress (τ) and rate of shear strain ($\dot{\gamma}$) for Newtonian fluid. This is not the case for non-Newtonian fluids where η is a function of τ and $\dot{\gamma}$ as well as multiple rheological parameters. The different non-Newtonian fluids are Power-law, Herschel-Bulkley, Bingham, Casson etc. The constitutive model equations for selected non-Newtonian fluids are shown in below table.

Table 1.1 Constitutive equations of non-Newtonian fluids

Type of non-Newtonian Fluid	Constitutive equation	Parameter
Power-Law	$\tau = K \dot{\gamma}^n$	Two Parameter
Bingham	$\tau = \tau_y + \mu_p \dot{\gamma}$	Two Parameter
Herschel-Bulkley	$\tau = \tau_y + K \dot{\gamma}^n$	Three Parameter
Casson	$\tau^{1/2} + (\mu_c \dot{\gamma})^{1/2}$	Two Parameter

Power-Law fluids do not contain the yield stress and they can be pseudoplastic (shear-thinning) or dilatants (shear thickening) depending on the flow behaviour index, n . The Herschel-Bulkley, Bingham, and Casson fluids shows the addition of a yield stress. In order to fluid to flow, the applied stress must exceed the yield stress.

1.3 Slurry Flow

Slurry is essentially a mixture of solids (Solid particle) and liquids (Carrier fluid). The most commonly used fluid is water, but attempts have been made to use crude oils with milled coal and even air in pneumatic conveying **Abulnaga (2002)**. Slurry flow in a pipeline is very much different from the single phase flow. It is possible to allow single phase liquid to flow at slow speed from a laminar flow to turbulent flow. However in two phase flow, such as slurry, one must overcome a deposition critical velocity. The physical characteristics of slurry are dependent on many factors such as size and distribution of particles, concentration of solids in the liquid phase, size of the conduit, level of turbulence, temperature and viscosity of the carrier. When we turn from flow of a simple liquid to that of a slurry, i.e a mixture of solid particles in a carrier fluid, the need immediately arises for a more precise system of nomenclature. For example, instead of a single density, ρ , several densities must be distinguished. These includes the density of the fluid, ρ_f , that of the solid particles, ρ_s and that of the mixture ρ_m .

In specifying concentration, care is required to distinguish between delivered and *in situ* values. The delivered concentration is the fraction of solid delivered from (or fed to) the conveying system. If slurry discharged from the system is collected in tank, then the volume fraction of solids for the mixture in this tank is the delivered concentration C_{vd} . On the other hand, the resident or *in situ* concentration is the average concentration present in the system means if the length of pipe were isolated by suddenly closing valves at both ends, then the volumetric fraction of solid in isolated pipe is the resident or in situ volumetric concentration C_{vi} .

Another area in which slurries require a more careful treatment than single-phase fluid is that of friction gradient or energy gradient. In the form of pressure gradient dp/dx , the friction loss

associated with the flow of slurry in a pipe is unambiguous. For a single fluid the hydraulic gradient is $(-dp/dx)/\rho g$. The possible ambiguity in the flow of slurry arises from the density to be used in this expression. Thus an alternative definition of the mixture hydraulic gradient is based on the mean density of delivered slurry is created which is given as:

$$j_m = \frac{1}{\rho_{md} g} \left(-\frac{dp}{dx} \right) \quad 1.2$$

The properties of slurries depend very strongly on the tendency of the particles to settle out from the conveying liquid. For transport of settling slurries an important parameter is the terminal velocity, v_t . Terminal velocity is the velocity at which a single particle settles through a large volume of liquid. The terminal velocity depends on the liquid properties (ρ_f and μ) on the particle diameter (d) and its density (ρ_s) and to lesser extent, on its shape **Abulnaga (2002)**. Generally particles in slurry are not spherical, but the sphere represents a convenient reference case in analysis. The weight of the particle is partially reduced by buoyancy of the surrounding fluid.

For slurries of very fine particles the tendency for the particles to settle out from the liquid can be neglected. As a result, the slurry can be treated for most purposes as a single phase fluid. In that case the delivered and *in situ* concentrations are identical, provided that the line is not left full of stagnant slurry for extended period, a stationary bed of solid does not form.

1.4 Classification of Flow Regimes

Based on the specific gravity of particles flow of nonsettling slurries is divided into four categories **Brennen (2005)**.

- Homogenous suspension for particles smaller than 40 μm .
- Suspensions maintained by turbulence for particle sizes from 40 μm to 0.15 mm.
- Suspension with saltation for particle sizes between 0.15 mm and 1.5 mm.
- Saltation for particles greater than 1.5 mm.

Due to interrelation between terminal velocity, deposition velocity and particle sizes the above classification has been modified to four flow regimes based on actual flow of particle and their size shown in fig. 1.2.

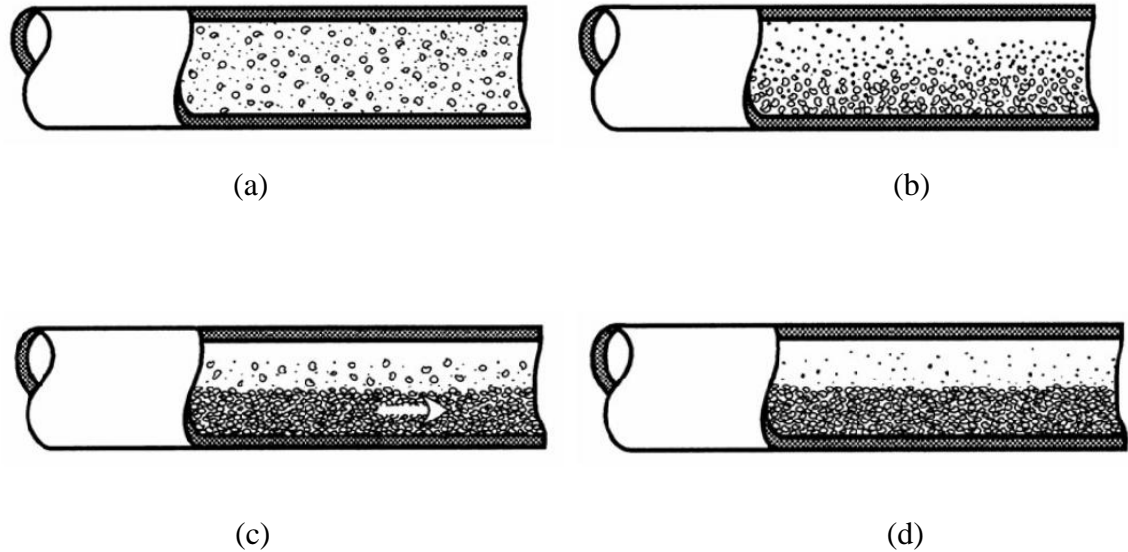


Fig. 1.2 Flow regimes for slurry flow in a horizontal pipeline. (a) Homogenous flow, (b) Heterogeneous flow, (c) Flow with moving bed, and (d) Flow over a stationary bed. **Brennen (2005)**

Two phase flow regime mainly depends on the flow rates, phase materials and pipe orientation. For liquid-solid flows, the particle diameter and solid mean concentration are often used to classify the nature of the mixture and flow regimes. The solid mean concentration is generally used to refer dilute or dense flow.

1.4.1 Classification based on particle size

On the basis of particle size solid-liquid slurry can generally be classified into two categories : homogenous and heterogeneous. Due to non availability of a clear cut distinction between homogenous and heterogeneous slurries, the flow in which the mean particle diameter is greater than 50 μm generally displays heterogeneous properties.

Heterogeneous slurries have more complicated flow behavior than homogenous slurries. These slurries are typically a mixture of coarser particles in a homogenous carrier fluid. Due to submerged weight and effects of gravity on the coarse particles, sedimentation occurs within

the flow. As a result, concentration and velocity profiles across the flow domain are non-uniform.

1.4.2 Classification based on solid concentration

For Newtonian heterogeneous flows, the solid concentration is often used as a criterion to determine when the flow is dilute or dense. If the motion of the particles is controlled by local hydrodynamic forces then the mixture is said to be dilute. In this case, the effects of particle-particle interactions may be neglected. For the case where the flow is controlled by both the hydrodynamic forces and particle-particle interaction, the mixture is considered to be dense.

There is no universal criterion for distinguishing between dilute and dense flows on the basis of concentration. The criterion varies from study to study and depends on the type of mixture and the flow structure under investigation. The physical characteristics of whether the flow is dilute or dense have been broadly classified into three categories on the basis of inter particle collisions 1) collision-free flow or dilute flow; 2) collision-dominated flow or medium concentration flow; and 3) contact-dominated flow or dense flow.

1.5 Critical Velocity and Hold Up

It is the minimum velocity at which the solids form a bed at the bottom of the pipe from fully suspended flow. It is the transition velocity between the heterogeneous flow and saltation flow. It is one of the most important parameter that designer must know accurately for the optimized design of a slurry transport pipeline. The main significance of this velocity is that it represents the lowest speed at which slurry pipelines can operate and corresponds to lowest pressure drop in slurry transport. In slurry pipeline different layers of solid moves with different speed. Hold ups are due to slip velocity of layer large particles. Thus when there is hold up of solid particles relative to fluid the in situ concentration is larger than the delivered concentration. The phenomenon of variation of in situ concentration from the delivered concentration is referred as Hold up. Hold up plays a vital role in failure of many empirical relations predicting head loss in flow regimes involving bed loss.

1.6 Pressure Drop

Design of slurry pipeline system involves the estimation of head loss and thus, the power requirement under various operating conditions. Several correlations for the prediction of Fanning friction factor are available in literature, which are mostly of empirical nature. These correlations have been developed based on rheological parameters and experimental data on multi-sized homogeneous slurries. Most of the developed equations have been based on limited data comprising of uniform or narrow size-range particles with very low to moderate concentrations. These correlations are prone to great uncertainty as one departs from limited database that support them.

1.7 Concentration and Velocity Profile

Wear, which is defined as volume loss of material from a surface due to abrasion, erosion or other causes, is a very important consideration in the design and operation of slurry system. It affects both the initial capital cost and the life of components. It has been indicated in the literature that wear is proportional to volume concentration and the velocity thus it is reasonable to assume that wear will depend on number of particle impacts on the surface, which depends on velocity and concentration. So it is important to know in detail about in situ velocity profiles and concentration profile of solid to understand the wear phenomenon.

1.8 Motivation of present work

Conveying solid through pipelines on large scale has now come to be accepted as a viable alternative to the conventional modes of transportation. Large number of slurry pipelines were already built around the world and lot more are still to come up. To design the pipeline, designers need accurate information regarding pressure drop, critical velocity, flow regimes etc. The need and benefits of accurately predicting velocity profiles, pressure drop, concentration profile of slurry pipeline during the design phase is enormous as it gives better selection of slurry pump, optimization of power consumption. It has been the endeavour of researchers around the world to develop accurate models. The major empirical equations regarding pressure drop, hold up, critical velocity and flow regime identification when tested

with experimental data of different systems collected from open literatures, it was found that prediction error ranges above 25% on average.

The motivation of the present work is to find the applicability of Computational Fluid Dynamics (CFD) in slurry flow modeling. The limitations of empirical equations based correlations are that they do not provide deeper insight of complex phenomena of slurry flow. In recent years with advancement in CFD techniques, CFD becomes a powerful tool for predicting fluid flow, heat/mass transfer, chemical reactions and related phenomenon by solving mathematical equation that govern these processes using a numerical algorithm on a computer. Considering the limitations in the published studies, the present work has been concentrated on a systematic development of CFD based model to predict the solid concentration profile, velocity profile and pressure drop in slurry pipeline.

There is a considerable research work that has been done in the past to predict the pressure drop, concentration profile and velocity profile for solid liquid slurry flow through pipeline. The precise knowledge of above mentioned parameters provides a great help in selection of slurry pump and hence improve power consumption. Various factors that effects the parameter such as pressure drop, velocity profile etc. have been investigated by numerous researchers. Majority of research done in past is focused on low or moderate concentration of solid particles. In the present study, prior to the research work an extensive review of the published works in the field of solid-liquid slurry transport with an emphasis on the effect of various factors like particle size distribution, solid loading, mixing of different sized particles that affects the pressure drop, concentration profile and velocity profile characteristics were undertaken and a review of published works are presented in this chapter.

Skudarnov et al. (2004) performed experiment on slurry transport of five double-species slurries composed of glass beads and water. The various combinations taken for double-species glass beads were consist of two different densities and three narrow particle size distribution. Pressure gradients for double-species slurries were compared to those for individual components at same solid volume fractions. Also, the effect of mean particle diameter on pressure gradient of double- species slurry in the pipe was studied. The test loop used for experimental study has internal pipe diameter of 23 mm. It has been concluded that an increase in the solid mean particle diameter results in higher pressure gradients for low velocities but lower pressure drop for high flow velocities and also the pressure gradient curve for double-species slurry is always between the curves for individual components.

Kaushal et al. (2005) conducted an experiment in 54.9 mm diameter horizontal pipe on two sizes of glass beads having mean diameter and standard deviation of 440 μm & 1.2 and 125 μm & 1.15, and mixture of two sizes in equal fraction by mass. Flow velocity was set up to 5 m/s and overall concentration up to 50 % by volume for each velocity.

The rig consist of 22 m long recirculating pipe loop, 200 l capacity slurry tank, 150 l capacity water tank, and a centrifugal pump to maintain the slurry flow. The slurry was supplied from slurry tank, where a mixer powered by electric motor mixes the water and solid particles mechanically. A 15 kW pump was used, which supplies $0.6 \text{ m}^3/\text{min}$ at 22 m head. They observed that the pressure drop at any given flow velocity for slurry of 125 μm increases with increase in concentration. The rate of increase in pressure with concentration is small at low velocities but it increases rapidly at higher velocities. The pressure drop for slurry of 440 μm at any given flow velocity increases with increase in concentration, but rate of increase is comparatively smaller at higher flow velocities. Pressure drop for mixture of two sizes is less for most of the observation at higher overall concentration.

Verma et al. (2006) have calculated the pressure drop across a 90° horizontal bend for the fly ash slurry. Fly Ash slurry has been taken at high concentration. The pressure drop across the bend has measured at five concentrations in range of 50-65% (by weight). The data from the experiment has been analyzed to obtain the relative pressure drop, bend loss coefficient. The pilot plant test loop was consist of closed circuit mild steel pipe test loop of 30 m length, pipe has a diameter of 53 mm. The pump is driven by an induction motor of 22 kw, 415 v and 40 A. A circular mild steel pipe bend having 90° turn angle and radius ratio of 5.6 was used to generate the pressure drop data experimentally. The solid material used was fly ash which has specific gravity of 2.06 and pH value of 7.1 at 60% solid concentration. The maximum and minimum particle sizes are 300 μm and 3 μm with 84.4% of particles are finer than 75 μm . They concluded from the study that : 1) The relative pressure drop across the pipe bend increases with increase in velocity and approaches a constant value at high velocity for all solid concentration. 2) The bend loss coefficient shows a reducing trend with increase in flow velocity for the slurry flow at all concentrations. 3) The permanent pressure loss coefficient for bends increases marginally with the increase in the flow velocity at all concentrations tested. 4) The flow disturbances downstream of the pipe bend result in additional losses and their contribution to permanent pressure loss.

Chen et al. (2009) have used an Eulerian multiphase approach based on kinetic theory of granular flow to simulate the flow of coal water slurries in horizontal pipe. To model turbulent two-phase flow with strong particle- particle interaction, the RNG k- ϵ turbulent model was incorporated in governing equations. The model was first validated with pressure gradient and concentration profile data from open literature, then validated with pressure gradient data from author's experiment. The effect of influx velocity, grain composition and total influx were numerically investigated and result have displayed some important slurry flow characteristics, such as constituent particle concentration distribution and velocity distribution as well as pressure gradients, which are difficult to display in experiment.

Eesa et al. (2009) conducted a numerical study using an Eulerian-Eulerian computational fluid dynamics (CFD) model for pipe transport of coarse particles in non-Newtonian carrier fluids. They have used positron emission particle tracking technique to obtain the particle velocity profile which was used to validate the predicted flow field. They have investigated the effect of various parameters on the flow properties. The variables studied were : particle diameter (2-9 mm), mean solid concentration (5-40 % v/v), mean mixture velocity (25-125 mm/s). The diameter of pipe was 45 mm and the length was much greater than the maximum entrance length. The Software package used for the simulation was ANSYS CFX. They concluded that except for the smaller particles, the velocity profile of the solid phase exhibited a significant degree of asymmetry which increased with particle size. Increasing the concentration also increase the pressure drop which is due to increase in particle-particle interaction.

Ekambara et al. (2009) have predicted the behavior of horizontal solid-liquid (slurry) pipeline flow using a transient three-dimensional (3D) hydrodynamic model based on kinetic theory of granular flows. Computational fluid dynamics (CFD) simulation results, obtained using a commercial CFD software package, ANSYS-CFX. The simulations were carried out to investigate the effect of solid volume concentrations (8 to 45%), particle size (90 to 500 μ m), mixture velocity (1.5 to 5.5 m/s), and pipe diameter (50 to 500mm) on local, time-averaged solid concentration profile, particle and liquid velocity profiles, and frictional pressure loss. The experimental and simulated results indicate that

the particles are asymmetrically distributed in the vertical plane with the degree of asymmetry increases with increasing particle size. The CFD model described here is capable of predicting particle concentration profiles for fine particle slurries where fluid turbulence is effective at suspending the particle.

Lahiri et al. (2009) developed a robust hybrid artificial neural network (ANN) methodology, which can offer superior performance for important process engineering problems. For efficient tuning of ANN meta-parameter, hybrid artificial neural network and genetic algorithm technique (ANN-GA) was incorporated in this method. The algorithm has been applied for prediction of critical velocity of solid liquid slurry flow. A comparison with selected correlations in the literature showed that the developed ANN correlation noticeably improved prediction of critical velocity over a wide range of operating conditions, physical properties, and pipe diameter.

Lahiri et al. (2009) proposed a few numbers of correlations for identification of four different regimes (namely sliding bed, salvation, heterogeneous suspension, and homogenous suspension) in slurry pipeline. Regime identification is important for slurry pipeline design as it is the prerequisite to apply different pressure drop correlations in different regimes. Based on the a databank of around 800 measurements collected from different literature , using vector machine (SVM) modeling a method has been proposed to identify the regime. The method incorporates hybrid support vector machine and genetic algorithm technique (SVM-GA) for efficient tuning of SVM meta-parameters. An average misclassification error (AARRE) of 0.03% has been showed by statistical analysis in the proposed method. A comparison with selected correlations in the literature showed that the developed SVM-GA method noticeably improved prediction of regime over a wide range of operating conditions.

Vlasak et al. (2009) experimentally investigated fluidic ash, bottom ash and sand slurries to study the effect of slurry composition and volumetric concentration on the flow behavior of slurries containing fine-grained and coarse-grained particles. Kaolin slurries with and without peptizing agent were used as carrier liquid for the sand slurries to compare the effect of Newtonian and non-Newtonian carriers. The study shows a time-dependent yield pseudo-plastic behavior of fluidic fly and fly/bottom ash slurries and

possibility of the flow reduction by mechanical treatment or by the arrangement of particle size distribution. Author uses the Bulkley-Herschel model to approximate the flow behavior of fluidic ash in the laminar region. In the turbulent region, the Wilson or Slatter models can be used. The effect of the size distribution of the sand slurry on the hydraulic gradient depends on the flow velocity. The coarse sand slurry reaches a higher hydraulic gradient than the fine sand slurry, the difference decreases with time.

Yingjie et al. (2009) studied the effect of solvent on the viscosity change of coal-oil slurry under high temperature–high pressure during heating. In this paper, Heating coal-oil slurry plays an important role in direct coal liquefaction. During the heating process, some physical and chemical properties and the viscosity of coal-oil slurry will be the changes. A self-manufactured rotary viscometer was designed to measure the viscosity of coal slurry at high pressure and high temperature. Two kinds of solvents such asanthracene oil, Shenhua recycled oil and Yanzhou coal were used. The results show that the viscosity of Yanzhou coal-anthracene oil and Shenhua recycled oil slurry decrease firstly with the decreasing of solvent viscosity, then increase with measuring temperature for the absorption and volatilization of the solvent in atmosphere. Both of them have a viscosity peak with increasing measuring temperature in atmosphere. During heating process, the Yanzhou coal-anthracene oil slurry has a viscosity peak at about 583 K under high pressure , while the Yanzhou coal-Shenhua recycled oil slurry does not have a viscosity peak, but coke deposits appear at 623 K and above, under high pressure. In addition, the viscosity–temperature characteristics of thermally treated coal-oil slurry at different temperatures are the same, both have a viscosity peak with increasing heating temperature at the same measuring temperature.

Chandel et al. (2010) presented report on rheological characteristics and pressure drop of mixture of fly ash (FA) and bottom ash (BA). The pilot test loop consist of 42 mm diameter pipe and 50 m long. The mixture was taken in the ratio of 4:1 for fly ash and bottom ash at high concentration above 50 % by weight. The effect of flow velocity at various concentrations on pressure drop has been analyzed. Then a pressure drop has been predicted using the rheological data in a straight pipeline of 42 mm diameter. Predicted result shows good agreement with the experimental result and has been

concluded that the pressure drop for any given concentration increase with increase in flow velocity

Lahiri et al. (2010) developed a generalized slurry flow model using CFD and utilize the model to predict concentration profile. Initially a three-dimensional model problem was developed to understand the influence of particle drag coefficient on solid concentration profile. Various drag correlations were incorporated into a two-fluid model (Euler-Euler) along with the standard k- ϵ turbulence model with mixture properties to simulate the turbulent solid-liquid flow in pipeline. The Eulerian-Lagrangian model, however, which simulates the solid phase as a discrete phase and thus allows particle tracking, is in principle more realistic. But after conducting number of simulation trials, author concluded that the number of dispersed particles that can be tracked within all the different commercial CFD software available is currently very limited. The computational model was mapped on to a commercial CFD solver FLUENT6.2. Data from **Kaushal et al. (2005)** was selected to validate the three dimensional simulation.

Lei et al. (2010) proposed a long distance pipeline transportation system with an additive feeding system suitable for restarting after more than a 24-hour shutdown. The aim of their investigation was to find suitable stabilizing additives for fly ash-water slurry to prevent sedimentation during an interrupted period of pipelining. Rheological characteristics and sedimentation stability of the slurry with the addition of four kinds stabilizing additives were measured. Additives used in this study were rhamsan gums (S-194, S-130), carboxymethyl cellulose (CMC), and xanthan gum (Vanzan). They confirmed that viscosity of the fly ash water slurries increases with increase in concentration of stabilizer. The concentration of stabilizing additives to give the same viscosity as untreated slurry were determined as 0.2 wt%, 0.2 wt%, 0.45 wt% and 0.3 wt% for S-194, S-130, CMC, Vanzan, respectively. As a dispersing additive, naphthalene sulfonate-formeldehyde condensate (NSF) was used to reduce the viscosity of fly-ash slurry. They mixed fly ash with deionized water .to give a fly ash concentration of 68 wt%. The concentration of dispersing additive (NSF) was set at 0.3 wt%/slurry. The viscosity of fly ash-water slurry with and without additives was measured using

rheometer with coaxial rotating cylinders. They Concluded that stability of slurry with S-194 is better than that of other additive.

Lu et al. (2010) discussed the effect of particle size distribution on flow pattern and pressure drop in pipeline flow of slurries. Author observed three distinct flow patterns for different particle size distribution at different velocities. They are fully stratified, partial stratified and fully suspended. Particle size distribution effects flow patterns significantly. Fine particles and medium particles which has smaller weight tend to be lifted up by the turbulent dispersive action of the carrier, therefore uniform flow pattern is easily obtained making the flow fully suspended. Whereas coarser particles are too heavy to be fully lifted. It is difficult for coarse particles to come into fully suspended even at high velocity of slurries. Solid particles contribute to the total friction of mixture flow in two ways, through mechanical friction and viscous friction.

Hossain et al. (2011) performed 3D numerical simulation to predict the deposition of particles flowing through a horizontal pipe loop consists of four bends. Software package used for simulation was FLUENT 6.2. In the numerical simulation, five different particle sizes have been used as secondary phases to calculate the multiphase effect and inter-particle interaction also been considered. The deposition of particles along the periphery of the pipe wall was investigated as a function of particle size and fluid velocity. The conclusion was made from the simulated result that near the upstream of the bend, maximum particle concentration occurred at the bottom of the pipe. However, downstream the bend the maximum particle concentration occurred at an angle of 60° from the bottom.

Kaushal et al. (2011) modified the model for composite and solid concentration profiles which was earlier developed by Kaushal and Tomita (2002) by taking into account the effect of particle size and efflux concentration. The modified model has been used to calculate the ratio of heterogeneously and homogeneously distributed portion of each particle size. The method is based on assumption that the total pressure drop in two-phase flow can be split into two parts excess pressure drop due to bed formation (heterogeneously distributed particles) and vehicle pressure drop (homogeneously

distributed particles). The total pressure drop due to bed particles is the sum of pressure drop due to each particle size in bed. The total pressure drop due to slurry is the sum of pressure drop due to vehicle and total pressure drop due to bed particles. Comparison of experimental data and predicted result shows that modified model gives better prediction than the other models available in literature.

Mazumdar (2011) performed Computational Fluid Dynamics (CFD) analysis in four different 90° elbows with air water two-phase flow. Air velocity was varied from 15.24-45.72 m/sec, whereas nine water velocities in the range of 0.1-10 m/sec were used in the study. The mixture model along with k- ϵ turbulence model was used to perform the analysis on commercial software FLUENT. Hexahedral mesh was used to discretized the domain, due to its capability in providing high-quality solution, with a fewer number of cells than comparable tetrahedral mesh. The mixture calculation was initialized with a low under relaxation factor of 0.2 for the slip, calculations were performed by combination of SIMPLE pressure-velocity coupling. The first order upwind discretization scheme was used for momentum, volume fraction, turbulent kinetic energy and turbulent dissipation rate. Pressure drop profiles and their respective cross-sectional pressure contour maps were presented for characteristic flow behaviors in multiphase flow.

Vlasak et al. (2011) done an experimental investigation of the flow behavior and pressure drop of dense complex slurries containing sand of different particle size distribution (five different monodisperesed and polydisperesed sands with mean diameters ranging from 0.20 to 1.40mm), stony dust(mean diameter of 8 μ m and 33 μ m), or clay conveyed in water. The slurries were tested using experimental pipeline loop with inner diameters of 17.5 and 26.8mm. The slurry concentration ranges from 6% to 40% for sand slurry, from 26% to 48% for stony dust slurry, and from 45% to 51% for stony dust-sand slurry. They had concluded that the coarse sand slurry reaches a higher hydraulic gradient than the fine sand slurry, and difference decreases with increase in velocity. The polydispersed sand slurries reach nearly the same value of hydraulic gradient as the fine sand slurry. The data analysis shows the non-Newtonian behavior of highly concentrated sand-kaolin slurry. When the carrier Kaolin slurry is peptized, the

hydraulic gradient in laminar region becomes markedly lower. The favorable effect vanishes in transitional and turbulent region.

Kaushal et al. (2012) simulated the pipeline slurry flow of fine particles at high concentration using Mixture and Eulerian two-phase models. They have used hexagonal grid and Cooper type non-uniform three-dimensional grid to discretize the domain and control volume finite difference method was used to solve governing equations. The modeling results were compared with experimental data collected in 54.9 mm diameter horizontal pipe. Experiments are performed on glass beads with mean diameter of 125 μ m for flow velocity up to 5m/s. The overall concentrations up to 50% (namely 0%, 30%, 40%, 50%) by volume has taken. The modeling results by both the models for pressure drop in the flow of water were found to be in good agreement with experimental data. For flow of slurry, Mixture model fails to predict pressure drop. However, Eulerian model gives fairly accurate prediction for both the pressure drop and concentration profiles at all efflux concentration and flow velocities. Most of the particles were dragged in central core of pipeline due to slip velocity between fluid and solid, resulting maximum concentration to occur away from the pipe bottom.

Kumar et al. (2012) numerically simulated the pipeline flow of slurry particles using Eulerian model. Coarser particles of 440 μ m mean diameter is conveyed by fluid at concentration up to 30% in 54.9 mm diameter pipe. To discretized the computation domain an unstructured, non-uniform grid was chosen and a control volume finite difference technique is applied to solve the governing equations. To obtain the precise numerical solution in fully developed turbulent flow, the RNG k- ϵ turbulent used with ASM model. The modeling results were compared with author's experiment data and results for the pressure drop in the flow of water were found to be in good agreement with experiment data.

Mazumder (2012) performed a Computational Fluid Dynamics (CFD) analysis in four different 90 degree elbows with air water two-phase flows. He has taken inside diameters of 6.35 mm and 12.7 mm of elbows with radius to diameter ratio (r/D) of 1.5 to 3. The combination of three different air velocities, ranging from 15.24 to 45.72 m/sec, and nine different water velocities in the range of 0.2-10.0 m/s, was taken. He has investigated the

pressure drop at two different upstream and downstream locations using empirical, experimental, and computational method. Mixture model and a commercial code, FLUENT is used for performing the CFD analysis. GAMBIT was used for creating three-dimensional 90 degree elbows. The geometries were then imported to FLUENT to simulate pressure drop. A straight pipe section of 54-50 times the pipe diameter was added at both upstream and downstream of the elbow. The comparison of CFD prediction with experimental data and empirical model outputs showed good agreement.

Xiuyuan et al. (2012) prepared high-quality petroleum coke-sludge slurry (PCSS) with low viscosity and good stability by adding sewage sludge into petroleum coke-water slurry (PCWS), and they conducted systematic investigation of the rheological properties of PCSS and PCWS along with the sewage sludge. The experimental result shows that the PCWS is a dilatant fluid and has inferior stability; sewage sludge is pseudoplastic fluid. Rheological properties were changed, when certain amount of sewage sludge is added into PCWS to obtain PCSS, from a shear-thickening property to a shear-thinning property. The static stability of PCSS was analyzed by water separation ratio. Result indicates that sewage sludge has a significant impact on the static stability of PCSS. The higher the sewage sludge amount, the better the static stability of the PCSS.

Bandyopadhyay et al. (2013) presented the Computational Fluid Dynamics (CFD) analysis for the flow of non-Newtonian and gas-non-Newtonian liquid through elbow. They have used the commercial software Fluent 6.3 for the simulation. They have used pseudoplastic power law model for the simulation of non-Newtonian liquid flow through elbows, and for the two phase flow they have employed Elurian-Elurian approach. They have verified the CFD analysis result with author's previously published experimental result. They have created geometries in Gambit 6.3 preprocessor. An unstructured tetrahedral mesh of order 4×10^3 - 3×10^4 was used for elbow. Fluent 6.3 was used to solve the governing equations. Their CFD simulation result predicted that : 1) In case of non-Newtonian liquid flow through elbows i) The maximum velocity is shifted towards the inner wall of the elbow. ii) The pressure is greatest at the outer wall furthest from the center of curvature and least at the inner wall nearest to center of curvature. This is due to centrifugal forces. 2) In case of gas-non-Newtonian liquid flow through

elbows simulation result predicts that : i) As the mixture enters to the elbow due to centrifugal action heavier dense phase that is liquid moves to the outer wall and lower density phase, air moves to the inner wall. ii) The static pressure profile of elbows show that for 45° elbow pressure drop is more comparing to the 135° elbow. Static pressure is high at outer wall as heavier density SCMC phase goes to outer wall due to centrifugal force and low at the inner wall when the air phase exits.

Capecelatro et al. (2013) performed a computation of liquid-solid slurries in horizontal pipe to investigate the complex multiphase flow dynamics above and below the critical deposition velocity. They combined eddy simulation framework with lagrangian particle tracking solver to account for polydispersed settling particles in a fully developed turbulent flow. The two phases are fully coupled via volume fraction and momentum exchange terms. A fully conservative immersed boundary method is employed to account for the pipe geometry on uniform Cartesian mesh. Author Simulate two cases, each with a pipe geometry and particle size distribution matching an experimental study from Roco & Balakrishnam, which consider a mean volumetric solid concentration of 8.4%. In first case they considers a Reynolds number based on the bulk flow of the liquid of 85,000, resulting in heterogeneous suspension of particles throughout the pipe cross-section. Statistics on the concentration and velocity of the particle phase for this case show excellent agreement with experimental results. In second case lower Reynolds number of 42,600 was taken, which leads to the formation of stationary bed of particles. They identified three distinct regions below critical deposition velocity, corresponding to rigid bed , a highly-collisional shear flow, and a freely-suspended particle flow.

Kaushal et al. (2013) determined experimentally the rheological characteristics of fly ash slurries at high concentration and then calculate the pressure gradient using CFD modeling with input parameters obtained on the basis of rheological tests conducted on fly ash slurries. Results obtained from CFD modeling were validated with experimental data collected in the present study on pilot plant loop test. Eulerian model, granular version has been used to model multiphase phenomenon. Comparison between predicted values and experimental values shows that Eulerian model gives fairly accurate results at all efflux concentrations and flow velocity. It has been found that at any given velocity

Specific Energy Consumption reduce up to 65% solid concentration and increase drastically with further increase in solid concentration.

Kaushal et al. (2013) numerically simulated the slurry flow through horizontal bend. The flow is simulated by implementing Eulerian two-phase model in Fluent software. They have chosen a hexagonal shape and cooper type non-uniform three dimensional grid to discretized the entire computational domain. For solving the governing equations they used control volume finite difference method. To verify the simulation result, the modeling results were compared with the experimental data collected in 53.0 mm diameter horizontal bend with radius of 148.4 mm for concentration profiles and pressure drops. The particles of silica sand have the median particle size of 450 μm . The geometric standard deviation σ_g for the particle used in the present study is found as 1.15. Simulation has done with various concentrations of silica sand ranging from 0% to 16.28% by volume and for each concentration flow velocity was varied from 1.78 to 3.56 m/s. They have concluded that CFD can predict the pressure drop with fair accuracy for slurry flow through horizontal 90 degree bend. But the CFD results begins to deviate from the measured values as the concentration increases. It was also observed that bend loss coefficient (k_t) reduces with increase in flow velocity, and decrease in efflux concentration. For the concentration distribution at bend they concluded that the concentration distributions are skewed towards the bottom and this skewness being higher for lower velocity of 1.78 m/s. At higher velocities of 2.67 m/s and 3.56 m/s, the concentration distribution is more uniform.

Nabil et al. (2013) attempted to develop slurry flow model using the computational fluid dynamic (CFD) technique for complete understanding and visualization of slurry flow behaviour. The model developed was used to predict concentration profile, velocity profile and their effect on pressure drop taking the effect of particle size into consideration. Eulerian-Eulerian multiphase model along with standard k- ϵ model with mixture properties has been used. The computational model was mapped on to a commercial (CFD) solver FLUENT 6.3. The geometry was meshed into approximately 1.5×10^5 tetrahedral cells. For pressure velocity coupling Phase coupled SIMPLE (PC-SIMPLE) algorithm was used. The first-order upwind discretization scheme was used for

the volume fraction, momentum equation, turbulent kinetic energy and turbulent dissipation rate and all the simulations were performed in double precision. It was found that the CFD software is capable to successfully model the slurry interaction and observed that the particles were asymmetrically distributed in the vertical plane with the degree of asymmetry increasing with increase in particle size because of gravitational effect.

Computational Fluid Dynamics (CFD) is a powerful tool that uses numerical methods and algorithms to model the real life behavior of fluids. It allows the optimization of design parameters without the need for the costly testing of multiple prototypes. It is also a powerful graphical tool for visualizing flow patterns that can give insight into flow physics that otherwise would be very difficult and costly to discover experimentally. Governing equations exist to model fluid behavior, but it is not always possible to apply them to many of complex flow patterns we see in the real world directly as there would be too many unknown variables. However, CFD involves creating a computational mesh to divide up real world continuous fluid into more manageable discrete sections. The governing equations for fluid flow can then be applied to each section individually, but as the properties of each section are linked to its neighboring sections, all the sections can be solved simultaneously until a full solution for the entire flow field can be found. As with everything, CFD is not without its limitations. Its accuracy or validity are dependent on different factors: the quality and appropriateness of mesh, the degree to which the chosen equations match the type of flow to be modeled, the interpretation of the result, the accuracy of the boundary conditions entered by the user or the level of convergence of the solution.

Now the main question that arises is that, How does CFD calculates the results? As we all know that physical aspects of any fluid flow is governed by three fundamental principles: 1) mass is conserved; 2) Newton's second law ($\text{force} = \text{mass} \times \text{acceleration}$); and 3) Energy is conserved. These fundamental physical principles can be expressed in the terms of basic mathematical equations, which in their most general form are either integral equations or partial differential equations. Computational fluid dynamics is the art of replacing the integrals or the physical derivatives in these equations with discretized algebraic forms, which in turn are solved to obtain *numbers* for the flow field values at discrete points in time and/or space or We can say that Computational fluid dynamics is one of the branch of Engineering, finding numerical solutions of governing equations **Anderson (1995)**. CFD solutions generally require

the repetitive manipulation of many thousands, even millions, of numbers, a task that is impossible without the aid of a computer. Thus, the instrument which has allowed the practical growth of CFD is the high-speed digital computers. Various software packages are available such as Fluent, CFX, CFDRC, Comsol, which can be used for simulation.

3.1 Various Discretization Techniques

Discretization is the process by which a closed-form mathematical expression, such as integral or differential equation involving function, all of which are viewed as having an infinite continuum of values throughout some domain, is approximated by analogous expressions which prescribes values at only a finite number of discrete points or volumes in the domain **Anderson (1995)**. Analytical solution of partial differential equations involve closed-form expression which give the variation of the dependent variables continuously throughout the domain. In contrast, numerical solutions can give answers at only discrete points in the domain, called grid points. Various discretization techniques used in CFD are shown in fig. below

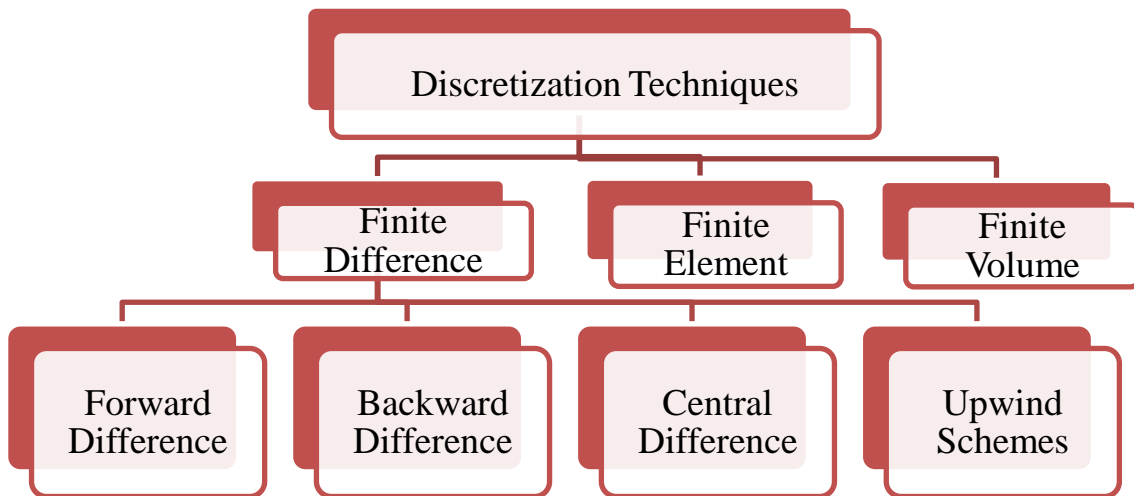


Fig. 3.1 Various discretization techniques

The stability of the chosen discretization is generally established numerically rather than analytically. It must be kept in mind that chosen discretization handles discontinuous solution gracefully.

3.2 CFD Analysis Steps

The rapid growth and research in field of CFD, its application and computation power have made possible the development of several commercial CFD codes such as FLUENT, CFX, STAR-CD. The complete CFD process in commercial software is basically divided into three parts namely Pre-processing, Solver and Post-processing. Fig. 3.1 shows complete CFD analysis procedure.

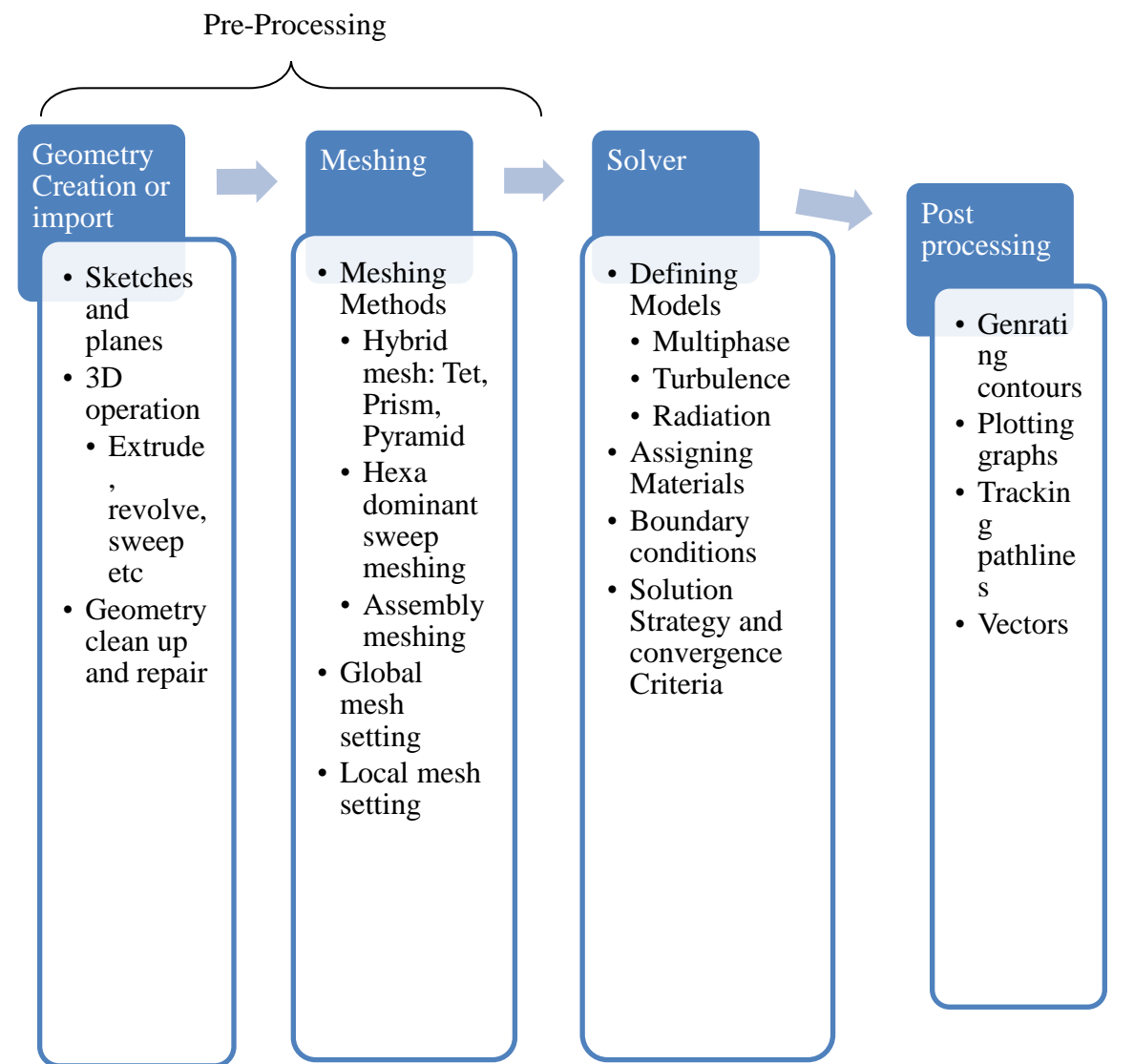


Fig. 3.2 CFD analysis steps

3.2.1 Pre processing

3.2.1.1 Geometry creation or import

Using specialized drawing tool the geometry of the flow domain is created. Usually, first the 2-D sketches are first drawn and then 3-D tools are used to generate the full geometry.

3.2.1.2 Mesh generation

In the mesh generation phase the continuous space of flow domain is discretized into sufficiently small discrete cells. The arrangement of these discrete cells determines the positions where the flow variables are to be calculated and stored. Gradient of variable is more accurately calculated on a fine mesh than on a coarse mesh. Therefore it is advisable to have fine mesh where large variations in the flow variables are expected. However a fine mesh requires more computational time and power. Mesh independence test is conducted to optimize the mesh size whereby, starting with a coarse mesh, the mesh size is refined until the simulation result is no longer affected.

3.2.2 Solver

This phase involves the defining of fluid and material properties, flow models (multiphase model, viscous model, radiation, energy equation etc), boundary condition and initial flow condition. Solution control and convergence criteria are also being set in this phase, which reflects the time taken and accuracy of the simulated result.

3.2.3 Post processing

In this phase the data obtained from the solver is visualized and displayed using a variety of graphical methods such as contour, plane, vector and line plots. Calculations can also be made to obtain the values of scalar and vector variables, such as velocity, pressure, etc. at different locations.

3.3 Advantages and Disadvantages of CFD

Advantages

Now a days, computational fluid dynamics (CFD) software developers focused on developing new model that can simulate liquid-solid flow to a much higher level of consistency. As a result, process industry engineers improve the model by evaluating alternative methods but it is too expensive or time consuming to trial on the plant floor. The use of CFD is helpful to engineers for obtaining solution problems regarding complex geometry and boundary conditions. A CFD analysis applicable for pressure, fluid velocity, temperature, phase concentration on a computational grid throughout the solution domain.

Disadvantages

- Physical models: The CFD solutions can only be as accurate as the physical model on which they are used.
- Numerical errors: numerical error when a problem is solving in computer
- Boundary conditions: when the initial/boundary conditions provided to the numerical model accurate then the CFD solution is as good as possible.

3.4 Applications of CFD

Applications of CFD is numerous, CFD is used in large number of industries for simulation such as :

- Aerodynamics of ground vehicles, aircraft and missiles.
- Heat transfer in industrial processes (Boilers, Heat exchangers, Combustion equipment, Piping etc.).
- Ventilation, heating and cooling flows in buildings.
- Heat transfer for electronic packaging applications and many more.

3.5 Multiphase Modeling

3.5.1 Approaches to multiphase modeling

There are two approaches for the numerical calculation of multiphase flow **Fluent (2011)**.

- Euler-Lagrange approach
- Euler-Euler approach

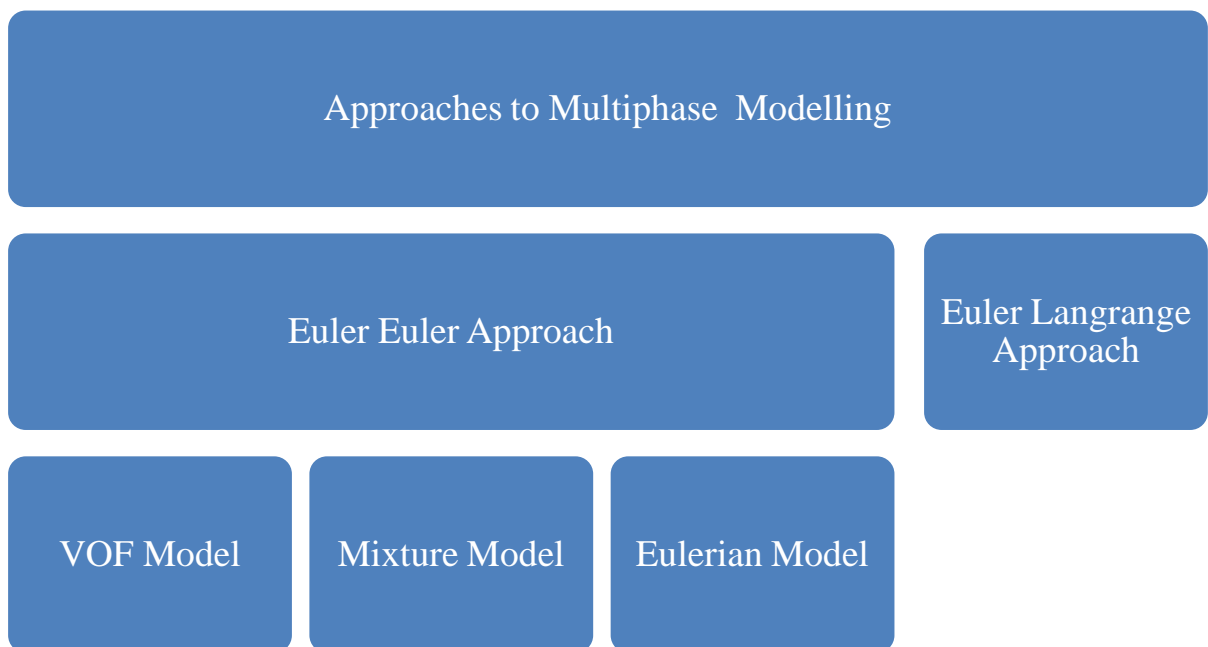


Fig. 3.3 Different approaches to multiphase modeling

1) The EULER-LAGRANGE Approach

The Lagrangian discrete phase model follows the Euler-Lagrange approach. The fluid phase is treated as a continuum in which fluid phase continuity and momentum conservation equations are solved in Eulerian framework using the time averaged Navier-Stokes equations with or without additional coupling terms, While the dispersed phase is solved by tracking a large number of particles, bubbles or droplets in the Lagrangian framework using Newton's second law. The dispersed phase can exchange momentum, mass and energy with the fluid phase.

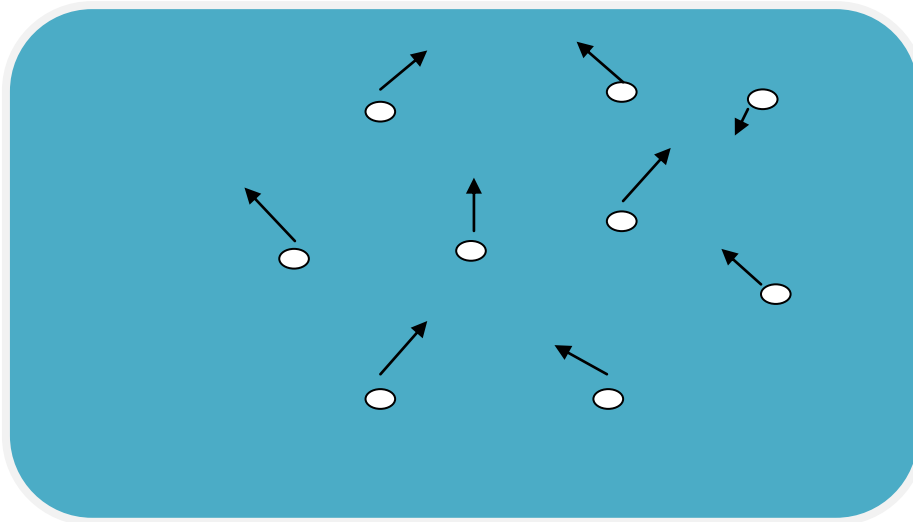


Fig. 3.4 Euler Lagrange approach visualization

This exchange takes place through coupling that can be one-way or two-way i.e the continuous phase can influence the dispersed phase flow or even the dispersed phase can influence the flow of continuous phase. The two frameworks are coupled through interaction forces implemented by considering the coupling mechanism between the fluid and the particles. This makes the model appropriate for the modeling of spray dryers, coal and liquid fuel combustion, and some particle laden flow, but inappropriate for the modeling of liquid-liquid mixtures, fluidize beds or any application where the volume fraction of second phase is not negligible. When the dispersed second phase occupies a low volume fraction, this approach can be made simpler when particle-particle interactions are neglected.

Trajectory of a discrete phase particle is predicted by integrating the force balance on particle. Force balance equates the particle inertia with the forces acting on the particle and can be written as

$$\frac{du_p}{dt} = F_D(\vec{u} - \vec{u}_p) + \frac{g(\rho_p - \rho)}{\rho_p} + \vec{F} \quad 3.1$$

$F_D(\vec{u} - \vec{u}_p)$ is the drag force per unit particle mass and F_D is given as

$$F_D = \frac{18\mu C_D Re}{\rho_p d_p^2 24} \quad 3.2$$

Here, \vec{u} is the fluid phase velocity, \vec{u}_p is the particle velocity, μ is the molecular viscosity of the fluid, ρ is the fluid density, ρ_p is the density of the particle and d_p is the particle diameter. Re is the relative Reynolds number given as

$$Re = \frac{\rho d_p |\vec{u}_p - \vec{u}|}{\mu} \quad 3.3$$

2) The EULER-EULER Approach

In the Euler-Euler approach the different phases are treated mathematically as interpenetrating continua and the RANS form of the continuity and momentum equations are solved for both the phases. Since the volume of a phase cannot be carried occupied by the other phases, the concept of the volume fraction is introduced.

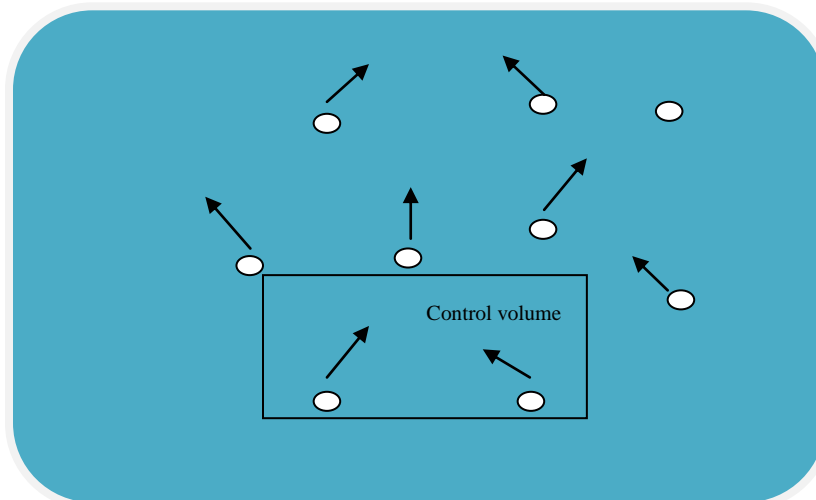


Fig. 3.5 Euler Euler approach visualization

These volume fractions are assumed to be continuous functions of space and time and their sum is equal to one. Conservation equations for each phase are derived to obtain a set of

equations, which have similar structure for all phases. These equations are closed by providing constitutive relations that are obtained from empirical information or in the case of granular flows by application of kinetic theory. There are three different Euler-Euler multiphase models.

- Volume of fluid (VOF) model
- Mixture model
- Eulerian model.

.1) The VOF Model

The VOF model is a surface-tracking technique applied to a fixed Eulerian mesh. It is designed for two or more immiscible fluids where the position of the interface between the fluids is of interest. This approach is particularly applicable for stratified or separated flow where a dispersed phase is well separated from the continuous phase with a distinct interface. The VOF formulation relies on the facts that two or more fluids are not interpenetrating. For each additional phase that we add in the model, a variable is introduced: volume fraction of the phase in computational cell. In the VOF model, a single set of momentum equations is shared by the fluids and the volume fraction of each of the fluids in each computational cell is tracked throughout the domain. The applications of VOF model include stratified flows, free surface flows, filling, sloshing, and the motion of large bubbles in a liquid

2) The Mixture Model

The mixture model is designed for two or more phases (fluid or particulate). The mixture model is a simplified multiphase model that can be used to model multiphase flows where the phases move at different velocities. It can also be used to model homogenous multiphase flow with very strong coupling. As in the Eulerian model, the phases are treated as interpenetrating continua. The mixture model solves for the mixture momentum equation and prescribes relative velocities to describe the dispersed phase. The mixture model is a good substitute for the Eulerian multiphase model in several cases. A full multiphase model may not be feasible when there is wide distribution of the particulate phase or when the interphase laws are unknown. Applications of the mixture model include particle-laden flows with low loading, bubbly flows, and sedimentation and cyclone separators. The mixture model can also be used

without relative velocities for the dispersed phase to model homogenous multiphase flow.

3) The Eulerian Model

The Eulerian model is the most complex of the multiphase models. It solves a set of N momentum and continuity equations for each phase. Couplings are achieved through the pressure and inter phase exchange coefficients. The manner in which this coupling is handled depends upon the type of phases involved; granular (fluid-solid) flows are handled differently than non- granular (fluid-fluid) flows. For granular flows, the properties are obtained from application of kinetic theory. Momentum exchange between the phases is also dependent upon the type of mixture being modeled. Applications of the Eulerian Multiphase Model include bubble columns, risers, particle suspension, and fluidized beds. The solution of the model is based on following:

- I. A single pressure is shared by all phases.
- II. Momentum and continuity equations are solved for each phase.
- III. The following parameters are available for granular phases :
 - Granular Temperature
 - Solid-phase shear and bulk viscosity

3.6 CFD Multiphase Model Formulation

In the present work Eulerian multiphase model is used where both liquid phase and solid phase are considered as interpenetrating continua. The Eulerian-Lagrangian model, which allows particle tracking, is in principle more realistic. After evaluating the relevant literature it is concluded that the number of particles that can be tracked by different commercial software is very limited, thus limiting the applicability of the Eulerian-Lagrangian model to only dilute mixtures.

3.6.1 Eulerian model

In the Eulerian-Eulerian approach two phases are considered mathematically as interpenetrating continua. The concept of volume fraction is introduced in this approach as the volume of one phase cannot be taken by another phase. The sum of volume fraction is equal to one i.e $\alpha_l + \alpha_s = 1$, where α_l and α_s are the volumetric concentration of solid and liquid phase. Here volume fraction represents the space occupied the each individual phase, mass and momentum conservation laws are satisfied by each phase individually.

1) Volume fraction equation

The volume of phase q, V_q , is defined as:

$$V_q = \int_V \alpha_q dV \quad (3.4)$$

Where

$$\sum_{q=1}^2 \alpha_q = 1 \quad (3.5)$$

2) Continuity equation

Continuity equation for phase q is given as :

$$\frac{\partial}{\partial t} (\alpha_q \rho_q) + \nabla (\alpha_q \rho_q \mathbf{v}_q) = \mathbf{0} \quad (3.6).$$

3) Momentum equation: For liquid phase

$$\frac{\partial}{\partial t} (\alpha_l \rho_l \vec{v}_l) + \nabla (\alpha_l \rho_l \vec{v}_l \vec{v}_l) = -\alpha_l \nabla p + \nabla \bar{\tau}_l + \alpha_l \rho_l \vec{g} + K_{sl} (\vec{v}_s - \vec{v}_l) \quad (3.7)$$

4) Momentum equation: For solid phase

$$\frac{\partial}{\partial t} (\alpha_s \rho_s \vec{v}_s) + \nabla (\alpha_s \rho_s \vec{v}_s \vec{v}_s) = -\alpha_s \nabla p - \nabla p_s + \nabla \bar{\tau}_s + \alpha_s \rho_s \vec{g} + K_{ls} (\vec{v}_l - \vec{v}_s) \quad (3.8)$$

Where α_l , v_l , ρ_l are the volume fraction, velocity and density of liquid phase and α_s , v_s , ρ_s are the volume fraction, velocity and density of solid phase. ∇p_s is a collisional solid stress that represent additional stresses in solid phase due to particle collision.

$$P_s = \alpha_s \rho_s \theta_s + 2\rho_s (1 + e_{ss}) \alpha_s^2 g_{o,ss} \theta_s \quad (3.9)$$

e_{ss} is the coefficient of restitution for particle collision taken as 0.9 and θ_s is a granular temperature which is directly proportional to kinetic energy of fluctuating particle. $g_{o,ss}$ is a distribution function, which shows the transition from compressible condition where spacing between the solid particles can continue to decrease to incompressible condition. After which no more decrease in spacing can occur. It is a correction factor that modifies the probability of collision between grains when solid granular phase become dense. It is given as :

$$g_{o,ss} = \left[1 - \left(\frac{\alpha_s}{\alpha_{s,max}} \right)^{\frac{1}{3}} \right]^{-1} \quad (3.10)$$

Where $\alpha_{s,max}$ is a packing limit.

$\bar{\tau}_s$ and $\bar{\tau}_l$ are phase stress tensor for solid and fluid which can be expressed as :

$$\bar{\tau}_s = \alpha_s \mu_s (\nabla \vec{v}_s + \nabla \vec{v}_s^{tr}) + \alpha_s \left(\lambda_s - \frac{2}{3} \mu_q \right) \nabla \cdot \vec{v}_s \quad (3.11)$$

$$\bar{\tau}_l = \alpha_l \mu_l (\nabla \vec{v}_l + \nabla \vec{v}_l^{tr}) \quad (3.12)$$

λ_s is the bulk viscosity of solid which accounts for the resistance of the granular particles to compression and expansion and it is given as:

$$\lambda_s = \frac{4}{3} \alpha_s \rho_s d_s g_{o,ss} (1 + e_{ss}) \left(\frac{\theta_s}{\pi} \right)^{1/2} \quad (3.13)$$

μ_s is the shear viscosity of solid which is defined as :

$$\mu_s = \mu_{s,col} + \mu_{s,kin} + \mu_{s,fr} \quad (3.14)$$

Where $\mu_{s,col}$, $\mu_{s,kin}$, $\mu_{s,fr}$ are the collisional viscosity, kinetic viscosity and frictional viscosity which are given as :

$$\mu_{s,col} = \frac{4}{5} \alpha_s \rho_s d_s g_{o,ss} (1 + e_{ss}) \left(\frac{\theta_s}{\pi} \right)^{\frac{1}{2}} \quad (3.15)$$

$$\mu_{s,kin} = \frac{10 \rho_s d_s \sqrt{\theta_s \pi}}{96 \alpha_s (1 + e_{ss}) g_{o,ss}} \left[1 + \frac{4}{5} g_{o,ss} \alpha_s (1 + e_{ss}) \right]^2 \alpha_s \quad (3.16)$$

$$\mu_{s,fr} = \frac{p_s \sin \phi}{2\sqrt{I_{2D}}} \quad (3.17)$$

Where ϕ is the angle of internal friction, and I_{2D} is the second invariant of the deviatoric stress strain tensor.

K_{sl} ($= K_{ls}$) is a liquid solid exchange coefficient different model are available for the K_{sl} expression depending on the solid volume fraction, the expression used in present study is given as **Fluent [2011]** :

$$K_{sl} = 150 \frac{\alpha_s(1-\alpha_l)\mu_l}{\alpha_l d_s^2} + 1.75 \frac{\rho_l \alpha_s |\vec{v}_s - \vec{v}_l|}{d_s} \quad (3.18)$$

3.7 Selection Criteria for Multiphase Model

The first step in solving any multiphase problem is to determine which of the regimes best represent the flow. General guidelines provides some broad guidelines for determining the appropriate models for each regime, and detailed guidelines provides details about how to determine the degree of interphase coupling for flows involving bubbles, droplets or particles, and the appropriate models for different amounts of coupling.

Dispersed phase volume fraction <10 %	<ul style="list-style-type: none"> • Discrete phase model (DPM)
Dispersed phase volume fraction >10 %	<ul style="list-style-type: none"> • Mixture model • Eulerian model
Pneumatic Transport	<ul style="list-style-type: none"> • Mixture model for homogenous flow • Eulerian model for granular flow
Slurry flow or hydrotransport	<ul style="list-style-type: none"> • Mixture model • Eulerian model

Fig 3.6 Guidelines for choosing multiphase model

In general, once that the flow regime is determined, the best representation for a multiphase system can be selected using appropriate model based on following guidelines **Fluent (2011)**. Additional details and guidelines for selecting the appropriate model are:

- For bubble, droplet and particle-laden flows in which dispersed-phase volume fractions are less than or equal to 10% use the discrete phase model.
- For slug flow, use the VOF model.
- For stratified / free-surface flows, use the VOF model.
- For pneumatic transport use the mixture model for homogenous flow or the Eulerian Model for granular flow.
- For fluidized bed, use the Eulerian Model for granular flow.
- For slurry flows and hydro transport, use Eulerian or Mixture model.
- For sedimentation, use Eulerian Model.

3.8 Turbulence Modeling

Whenever turbulence is present in certain flow it appears to be dominant over all other flow phenomenon. That is why successful modeling of turbulence greatly increases the quality of numerical simulations.

3.8.1 Complexity of turbulence modeling

Complexity of different turbulence models may vary strongly depends on the details one wants to observe and investigate by carrying out such numerical simulations. Complexity is due to the nature of Navier-stokes equation (N-S equation). Navier-stokes equation is inherently nonlinear, time dependent, three-dimensional PDE **Wilcox (2005)**.

Turbulence could be thought of as instability of laminar flow that occurs at high Reynolds number (Re). Such instabilities origin from interaction between non-linear inertial terms and viscous terms in N-S equation. These interactions are rotational, fully time-dependent and fully three-dimensional. Rotational and three dimensional interactions are mutually connected via vortex stretching. Vortex stretching is not possible in two dimensional space. Furthermore turbulence is thought of as random process in time. Therefore no deterministic approach is possible. Another important feature of turbulent flow is that vortex structure moves along the flow. Their lifetime is usually very long. Hence certain turbulent quantities cannot be specified as local. This simply means that upstream history of the flow is also of great importance.

3.8.2 Classification of turbulent models

Nowadays turbulent flows may be computed using several different approaches. Either by solving the Reynolds-averaged Navier-stokes equation with suitable models for turbulent quantities or by computing them directly. The main approaches are shown in fig. below

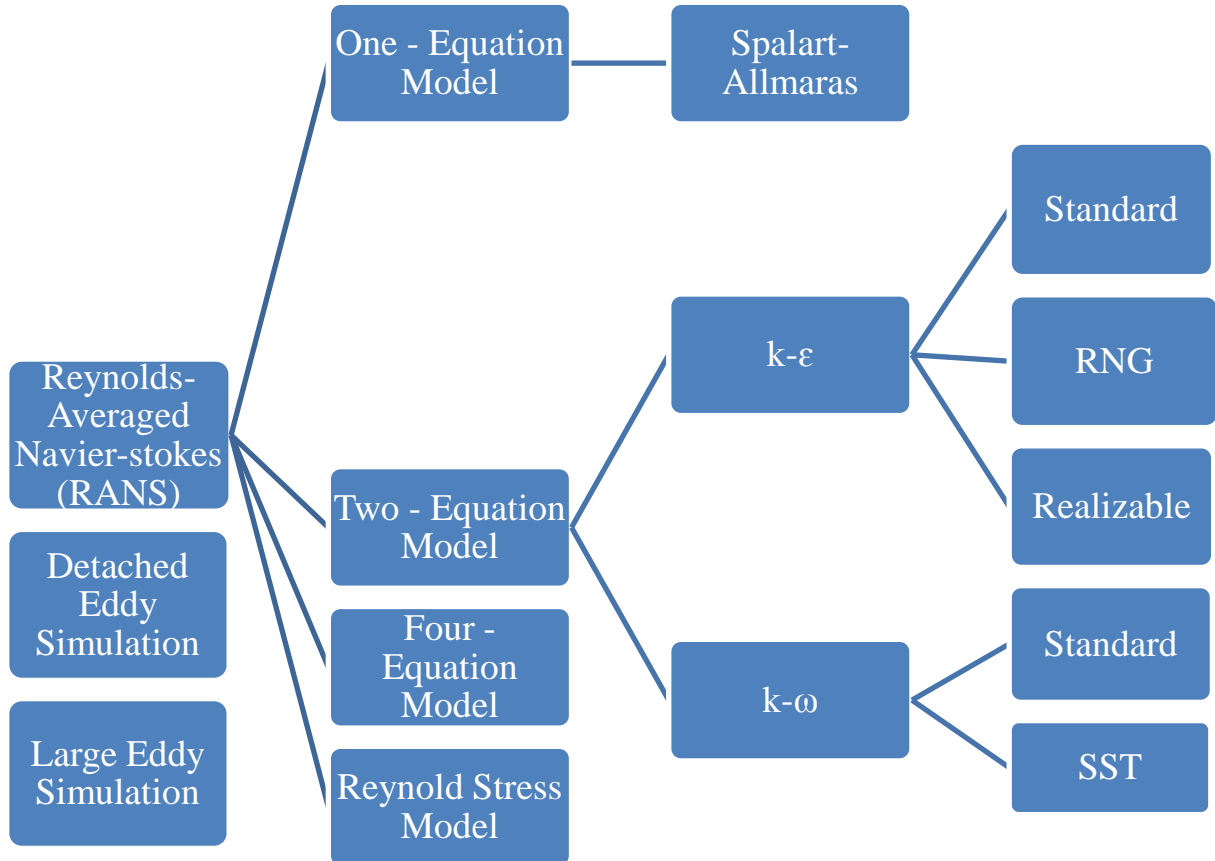


Fig. 3.7 Various Turbulence Model

3.8.3 Guidelines for selecting RANS turbulence model

Selecting Turbulence model for a particular problem greatly effects the result of the simulation. So some of the guidelines regarding selection of turbulence model for a particular problem is discussed in table 3.1.

Table 3.1 Selection of Turbulence Model

Model	Behaviour and Usage
Spalart-Allmaras	Economical for large meshes. Poorly performs for 3D flows and flows with strong separation. Suitable for 2D external/internal flows and boundary layer flows.
Standard k- ϵ	Widely used despite the known limitations of model. Poorly performs for complex flows involving severe pressure gradient, separation.
Realizable k- ϵ	Suitable for complex shear flows involving rapid strain, moderate swirl, locally transitional flow(e.g. boundary layer separation, vortex shedding behind bluff bodies, room ventilation).
Standard k- ω	Superior performance for wall bounded boundary layer, low Reynolds number flow. Suitable for complex boundary layer flow under adverse pressure gradient and separation (external aerodynamics and turbomachinery)
SST k- ω	Offers same benefits that of Standard k- ω , but dependencies on wall distance make this less suitable for free shear flow.
RSM	Suitable for complex 3D flows with strong streamline curvature, strong swirl/rotation (e.g curved duct, swirl combustors, cyclones)

4.1 Modeling and Meshing

.ANSYS Design Modeler (DM) is used to construct geometry. Geometry consists of pipe with internal diameter of 42 mm and length of 7 m shown in fig. 4.1 and 4.2. Length of the pipe is large enough, so that the flow is fully developed.

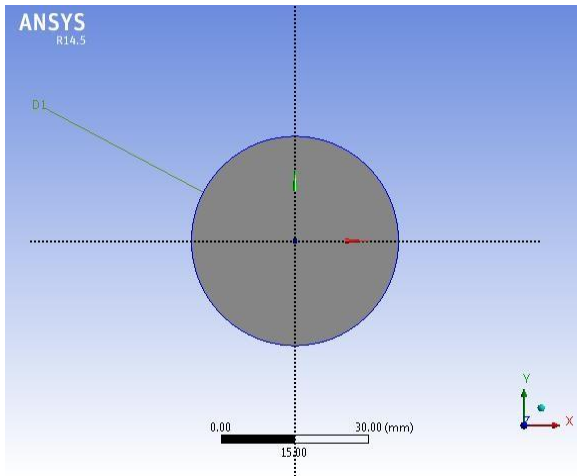


Fig. 4.1 Crosssectional View of Pipe (dia.: 42 mm)

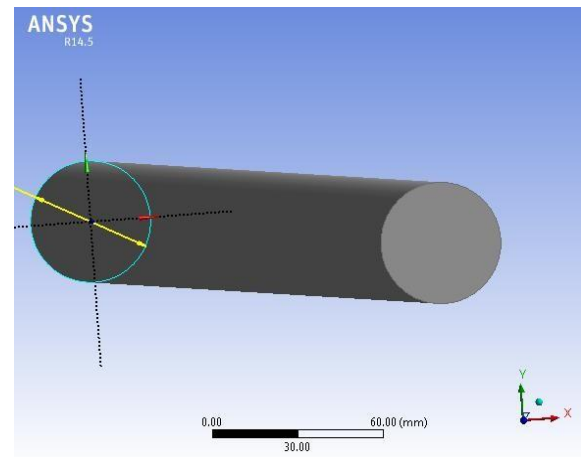


Fig. 4.2 Isometric view of Pipe (length 7 m)

Complete domain is discretized or mesh or grid is generated using Ansys ICEM tool. Four different geometries having different number of elements (230000, 332000, 415670, 565322, 630558) is generated to make the solution grid independent. Initially carrier liquid (water) is used to simulate the fluid flow from the pipe with different mesh size geometries and it is observed that after 415000 elements the solution becomes grid independent. All the four geometries with different mesh elements are shown in fig. 4.3 to 4.6.

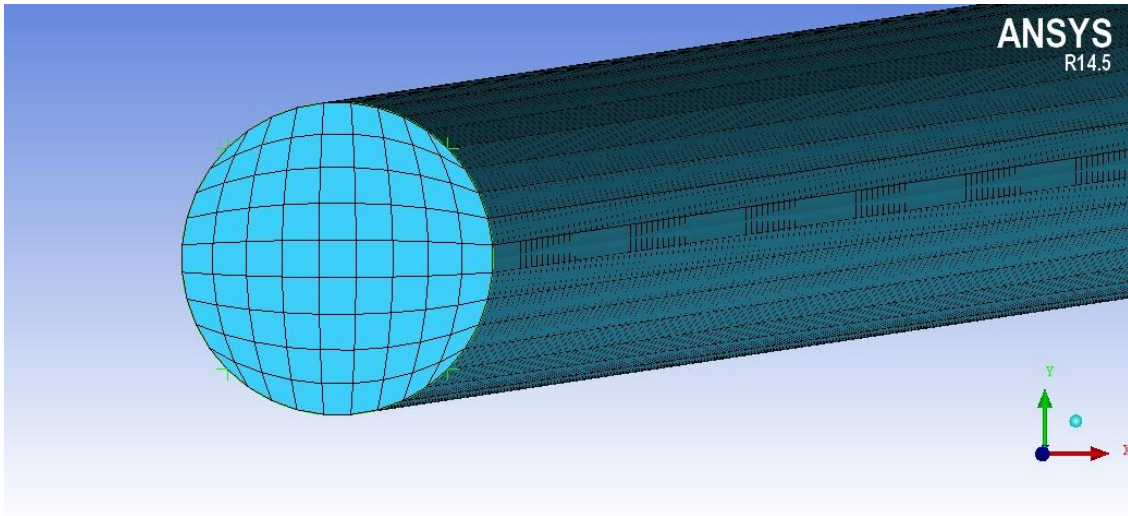


Fig. 4.3 Pipe mesh with 230000 number of elements.

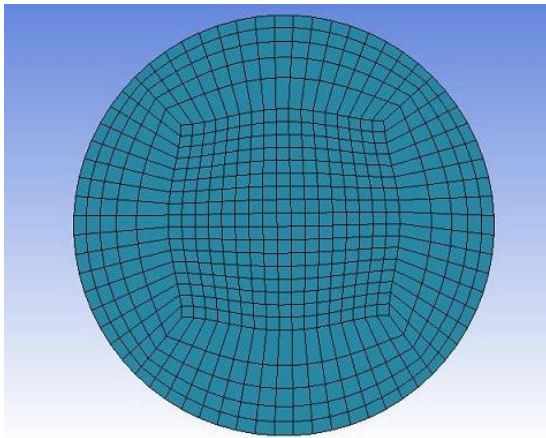


Fig. 4.4 Mesh with 332000 elements

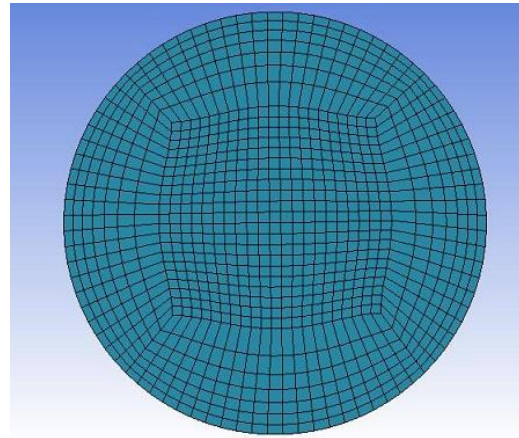


Fig. 4.5 Mesh with 415670 elements

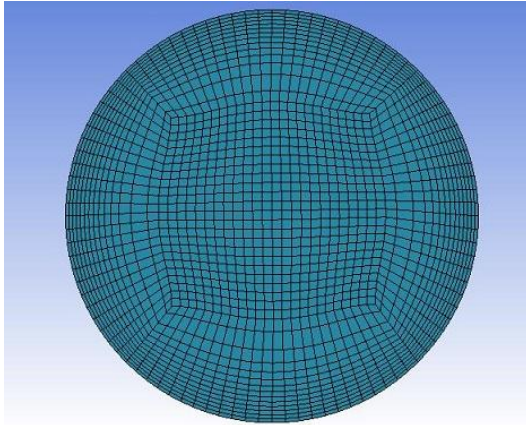


Fig. 4.6 Mesh with 565322 elements

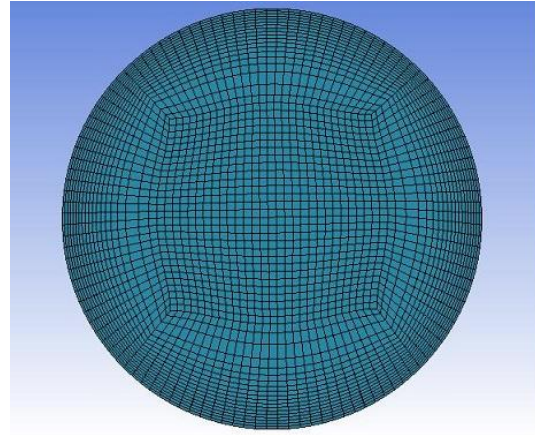


Fig. 4.7 Mesh with 630558 elements

Table 4.1 Grid independence of the simulation result

Number of elements	Inflation layer	Result variation with number of elements
230000	No	-----
332000	Yes	Yes
415670	Yes	Yes
565322	Yes	No
630558	Yes	No

First the mesh is generated without any inflation, but as we know that the properties are largely affected near the wall so inflation layers are added which give more fine mesh near the wall of the pipe to capture the boundary layer and variation in the properties.

4.2 Properties of Material

Rheological property of zinc and lime slurry at different concentration is shown in table below:

Table 4.2 Rheological properties of zinc water slurry with specific gravity of zinc 2.844

% concentration by weight	Temperature	Relative Viscosity	Water Viscosity (cP)	Slurry Viscosity (cP)	Flow Behaviour
30	25	1.8	0.98	1.764	Newtonian
40	25	2.4	0.98	2.352	Newtonian
50	25	4.3`	0.98	4.214	non-Newtonian
60	25	11.1	0.98	10.878	non-Newtonian

Table 4.3 Rheological properties of lime water slurry with specific gravity of lime 2.32

% concentration by weight	Temperature	Relative Viscosity	Water Viscosity (cP)	Slurry Viscosity (cP)	Flow Behaviour
30	25	1.8	0.98	1.764	Newtonian
40	25	2.4	0.98	2.352	non-Newtonian
50	25	5.8	0.98	5.684	non-Newtonian
60	25	15.8	0.98	15.484	non-Newtonian

4.3 Boundary Condition and Solution Strategy

Different boundary conditions and other inputs used in the numerical simulation of the slurry flow through pipeline is listed in table 4.4

Table 4.4 Inputs for simulation in FLUENT

Category	Discription	Input
Model	Multiphase Model	i) Eulerian model ii) No of phases : 2
	Viscous Model	i) k- ϵ turbulence, standard ii) standard wall function iii) dispersed properties.
Phase Properties and Interaction	Phase 1 (Primary)	Water
	Phasse 2 (Secondary)	Zinc talling, (Granular)
		Limestone, (Granular)
	Particle Diameter	33 μm (Zinc talling) 33 μm (Limestone)
	Granular Viscosity	Syamlal-Obrien
	Granular Bulk Viscosity	Lun-et-al
Phase Interaction	Syamlal-Obrien	
Operating Conditions	Operating Pressure	101325 pa
	Gravitational Acceleration	-9.81 m/s^2 in negetive y direction
Boundary Conditions	Inlet	Velocity inlet normal to boundary with constant value for both phases and constant volume fraction for secondary phase.
	Outlet	Pressure outlet with 0 gauge pressure with constant backflow volume fraction
	Wall	No-slip at wall

Solution Control	Pressure Velocity Coupling	PC-SIMPLE
	Momentum	First order upwind
	Volume Fraction	First order upwind
	Turbulent Kinetic Energy	First order upwind
	Turbulent Dissipation Rate	First order upwind

Simulation of two phase slurry flow through pipeline is carried out using Eulerian-Eulerian multiphase model along with standard k-ε turbulent model having standard wall treatment with dispersed multiphase properties. Carrier fluid (primary phase) used is water and the dispersed material used is limestone(sp. gravity 2.320) and zinc talling (sp. gravity 2.844). Boundary conditions for inlet and outlet are given as velocity inlet and pressure outlet with 0 gauge pressure at outlet and No-slip condition is defined at wall. Velocity used for simulation ranges from 1 to 3 m/s (1, 1.5, 2, 2.5, 3, 3.5 m/s) and concentration of solid ranges from 30 to 60 % by weight(30, 40, 50, 60). PC-SIMPLE algorithm is used for pressure velocity coupling and first order upwind scheme is used for discretizing momentum, volume fraction, turbulent kinetic energy and turbulent dissipation rate equations. Convergence criteria for continuity, momentum equations, turbulent kinetic energy (k) equation and turbulent dissipation rate (ε) equation is taken as 10^{-4} .

To check the grid independence of the result, first simulation is performed using carrier fluid (water) only on five pipes having same dimensions but different number of elements.. It is observed that after 415670 elements the result is no longer varies with number of element and hence grid independent.

4.4 Validation of CFD Simulation

Before starting simulation on desired slurry (Zinc slurry, lime slurry) first the results are validated with experimental data taken from **Chandel et al. (2010)** in which coal ash slurry is transported through pipeline. Mixture of fly ash and bottom ash in the ratio (4 :1) having specific gravity of 2.010 and weighted mean diameter of $d_{wm} = 85 \mu\text{m}$ was transported through pipeline. The results are very close to experimental data upto concentration of 65 % by weight after which it starts deviating and shown in figure 4.7

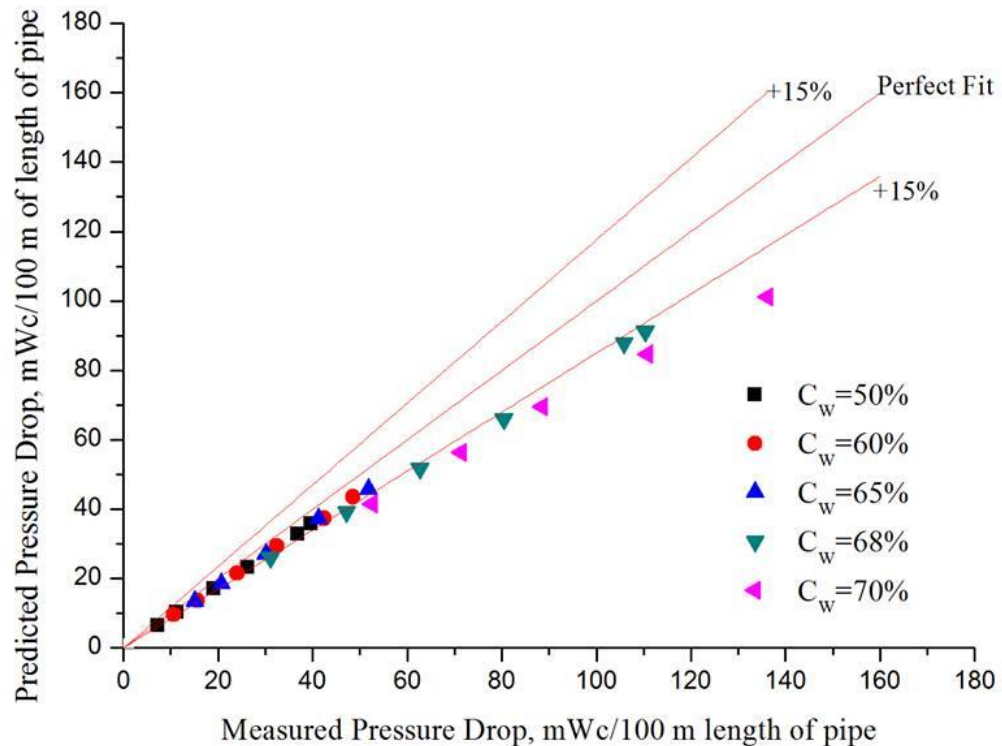


Fig. 4.7 Comparison between measured and predicted pressure drop at various concentration

It is clearly shown in above figure that numerical simulation results are in full agreement with an experimental data upto 65% concentration and after that it starts deviating. After validating the result of simulation, simulation is performed on zinc slurry and lime slurry which is the main objective of the thesis and various contours such as solid concentration profile contour, velocity profile contour has been generated.

4.5 Result and Discussion

4.5.1 Pressure Drop and Power Consumption

It is observed that the pressure drop increases with increase in the velocity as well as the concentration of the solid particles in the slurry. At low velocities the pressure drop increase slowly but it drastically increase at high velocities and hence the power required to transport the slurry. It is observed that for fine particles at higher velocity, pressure drop is large as compare to at low velocity which is due to increase in friction as the surface area is increased. Pressure drop and power required at various concentration and velocities for zinc slurry is shown in figure 4.8(a), 4.8(b) and for lime slurry is shown in figure 4.9(a), 4.9(b).

4.5.1.1 Zinc slurry

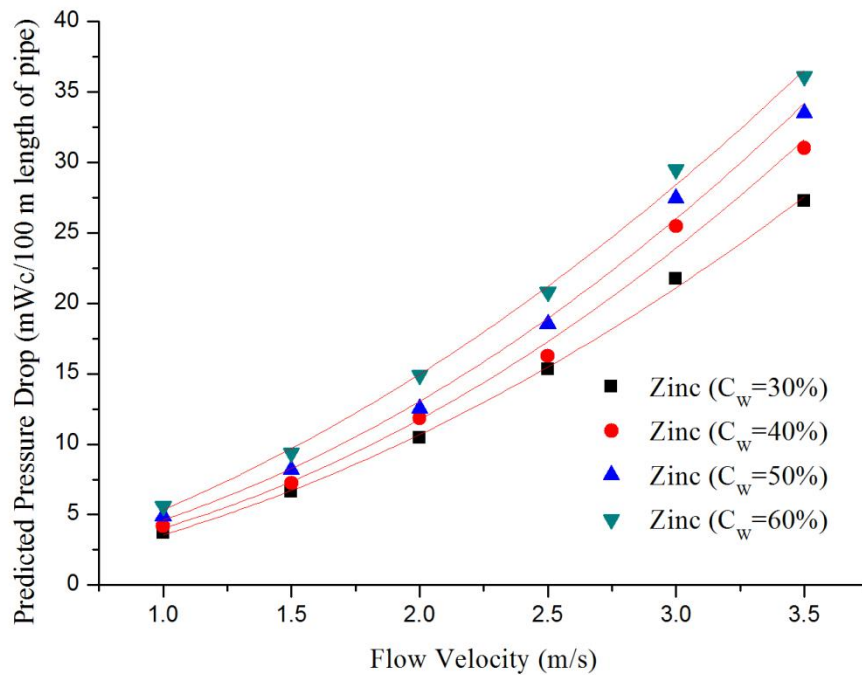


Fig. 4.8(a) Pressure drop comparison at different concentration for zinc slurry

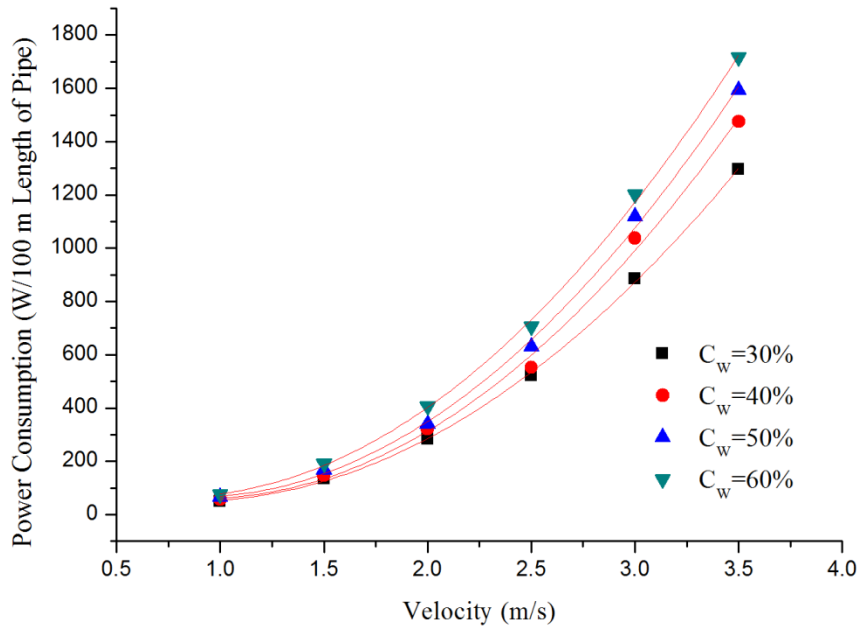


Fig. 4.8(b) Power consumption at various concentrations and velocities for zinc slurry

4.5.1.2 Lime slurry

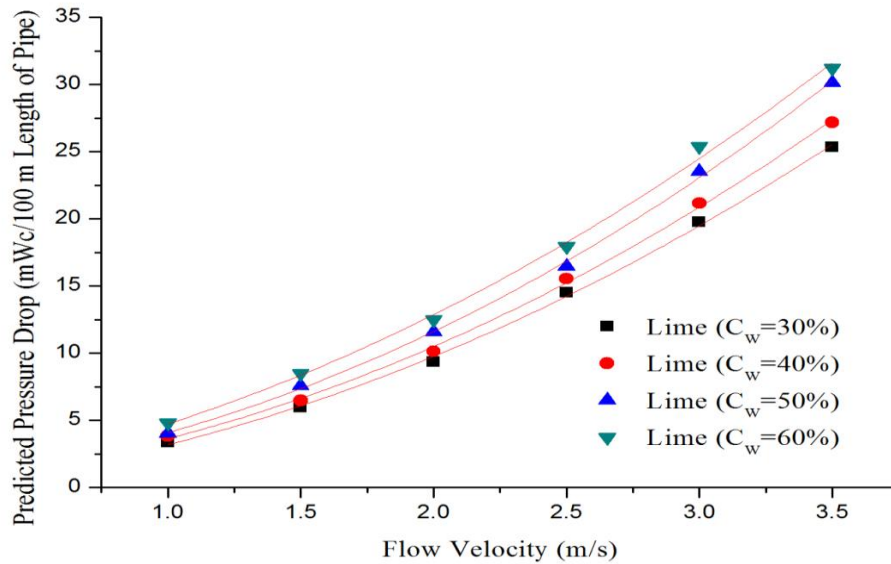


Fig. 4.9(a) Pressure drop comparison at various concentrations for lime slurry

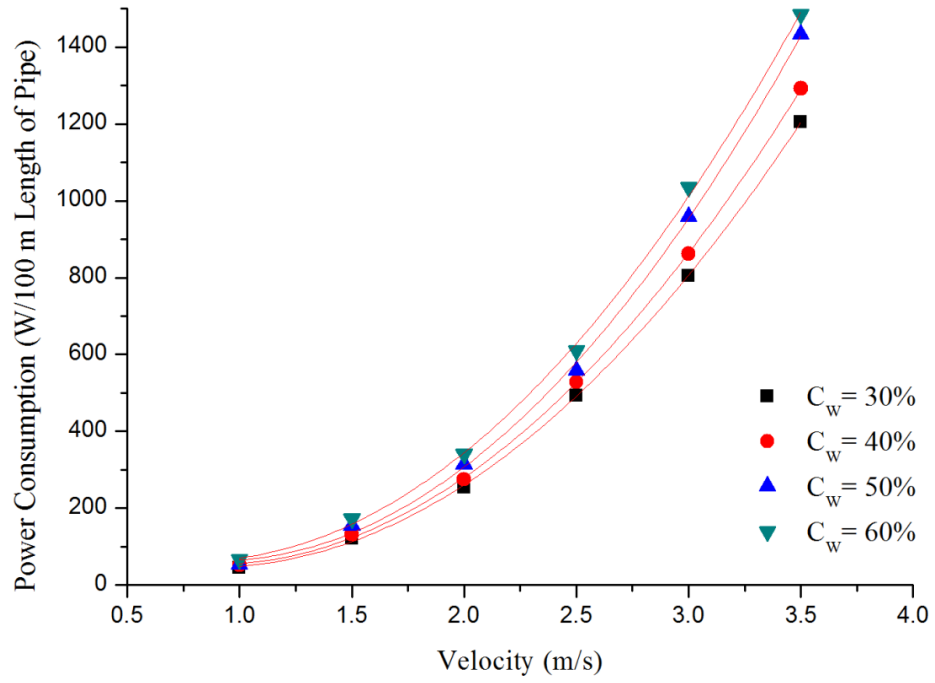


Fig. 4.9(b) Power consumption at various concentrations and velocities for lime slurry

4.5.2 Concentration Profile for Zinc Slurry and Lime Slurry

The CFD predicted vertical concentration profile of zinc slurry at the outlet of the pipe at various velocities and concentrations is shown in fig. 4.9 and that of lime is shown in fig. 4.10. As the particle size used in present simulation for the zinc is below $75\mu\text{m}$ ($33\mu\text{m}$) the flow is homogenous flow in which solid particle are fully mixed with carrier fluid as shown in below figures only small proportion of the solid particle are settled at low velocities which are again lifting up with increase in the velocity of the flow due to increase in turbulent energy which make particles suspended

4.5.2.1 Concentration profile of zinc slurry

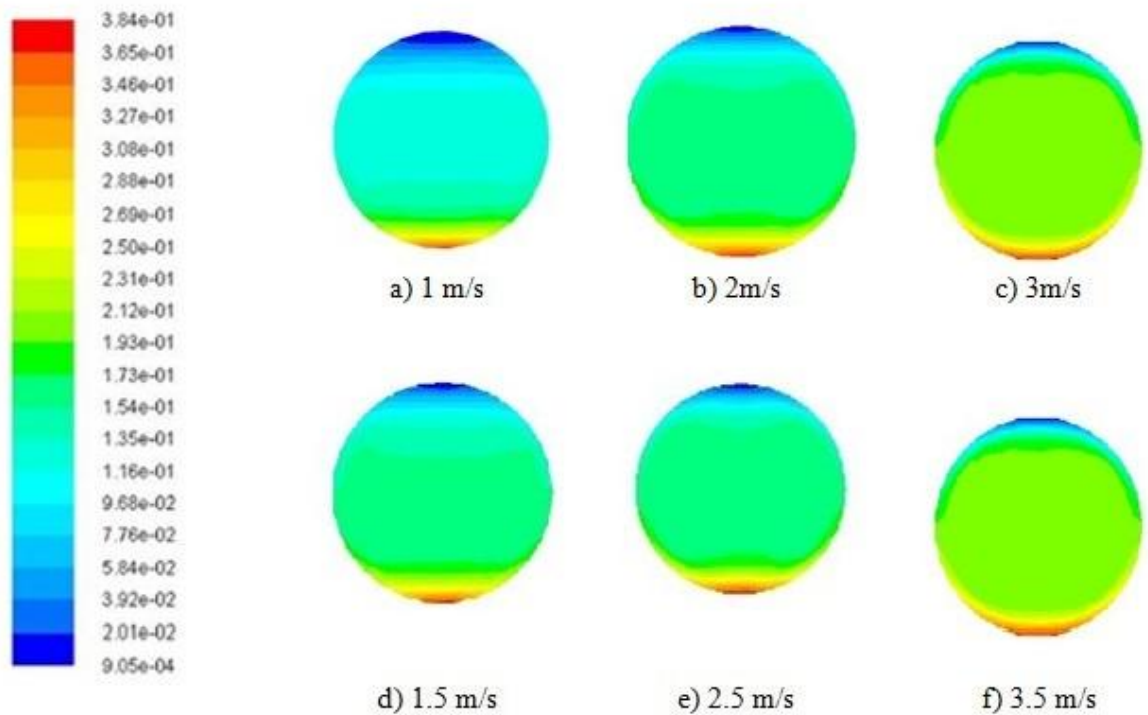


Fig. 4.10 (i) CFD predicted solid volume fraction contour at 30% concentration by weight at different velocities.

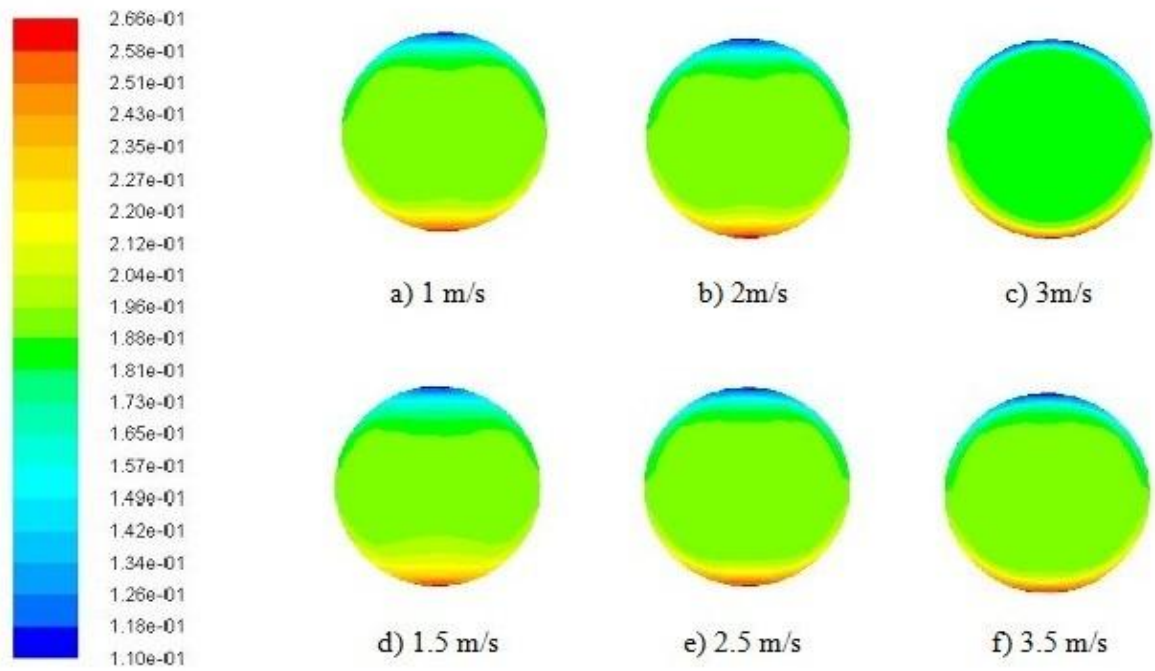


Fig. 4.10 (ii) CFD predicted solid volume fraction contour at 40% concentration by weight at different velocities.

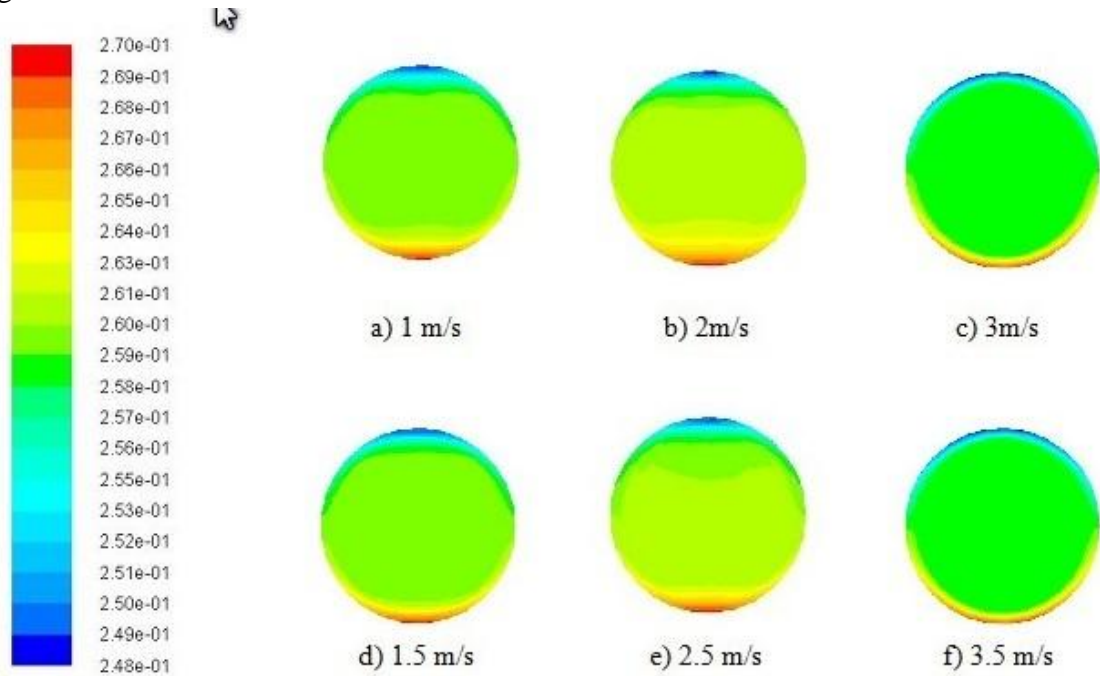


Fig. 4.10 (iii) CFD predicted solid volume fraction contour at 50% concentration by weight at different velocities.

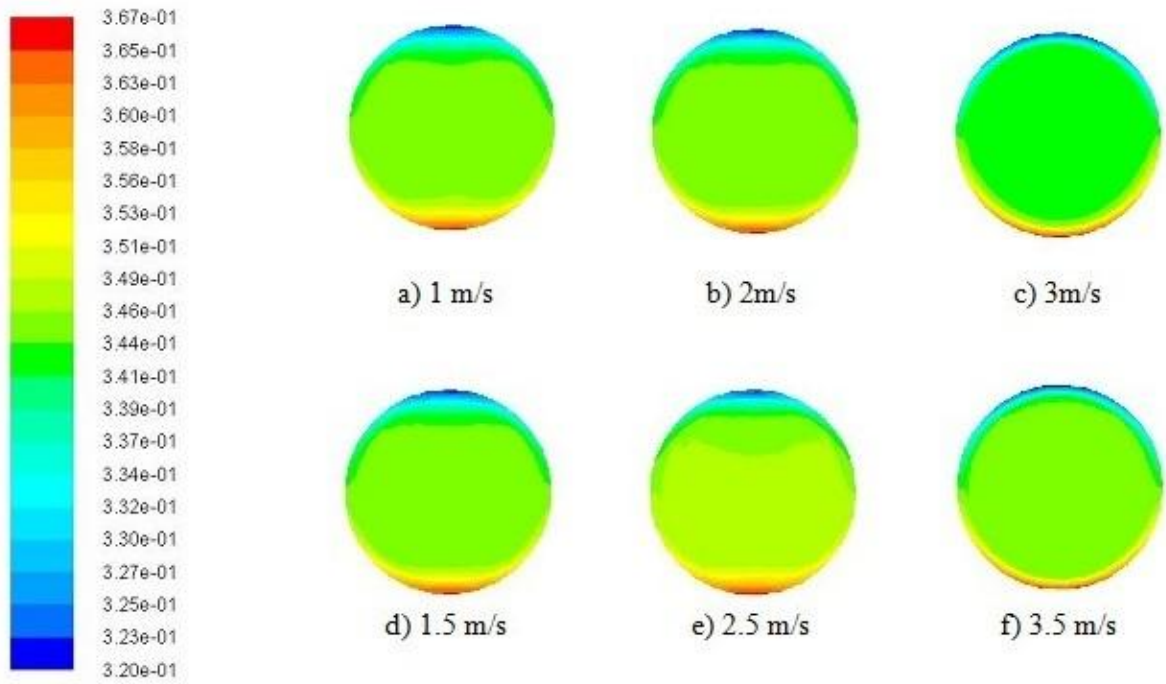


Fig. 4.10 (iv) CFD predicted solid volume fraction contour at 60% concentration by weight at different velocities.

4.5.2.2 Concentration profile for lime slurry

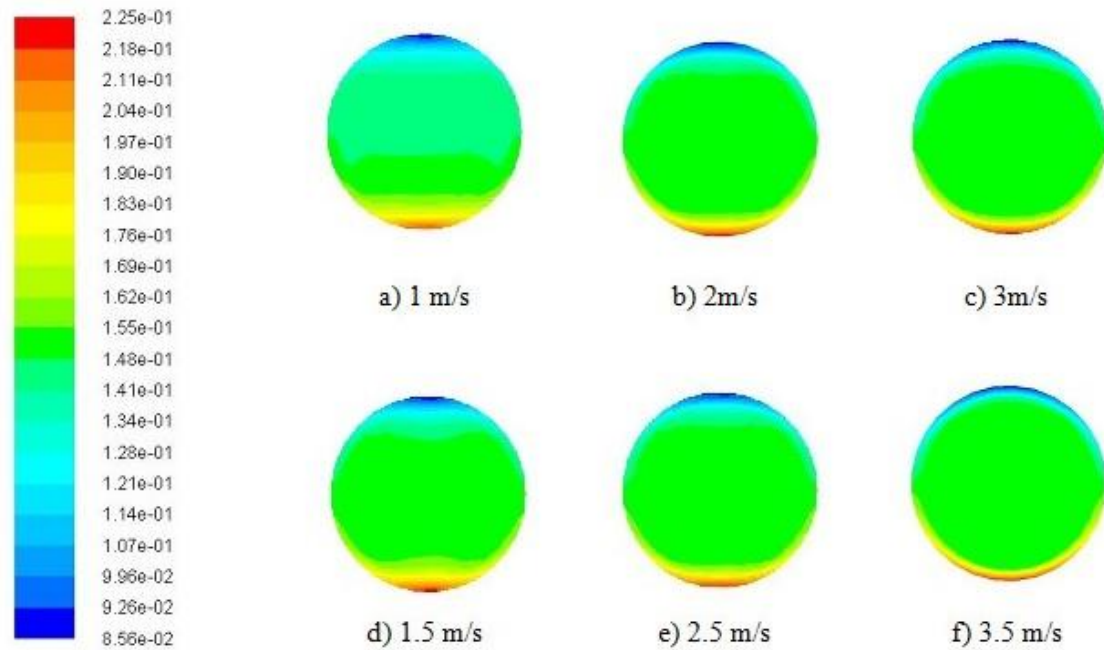


Fig. 4.11 (i) CFD predicted solid volume fraction contour at 30% concentration by weight at different velocities.

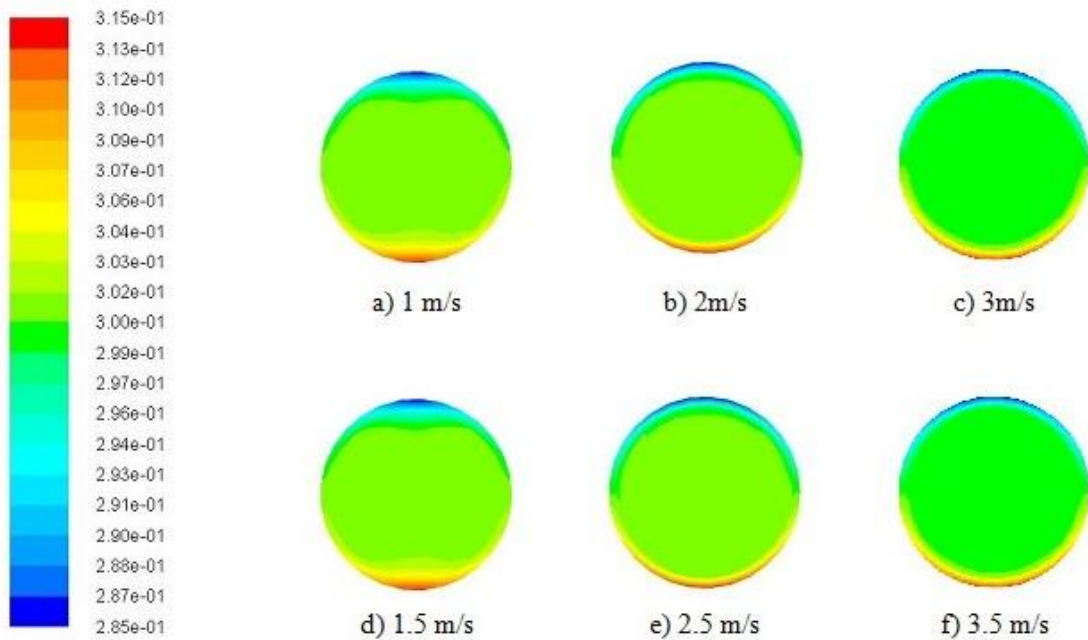


Fig 4.11 (ii) CFD predicted solid volume fraction contour at 50% concentration by weight at different velocities

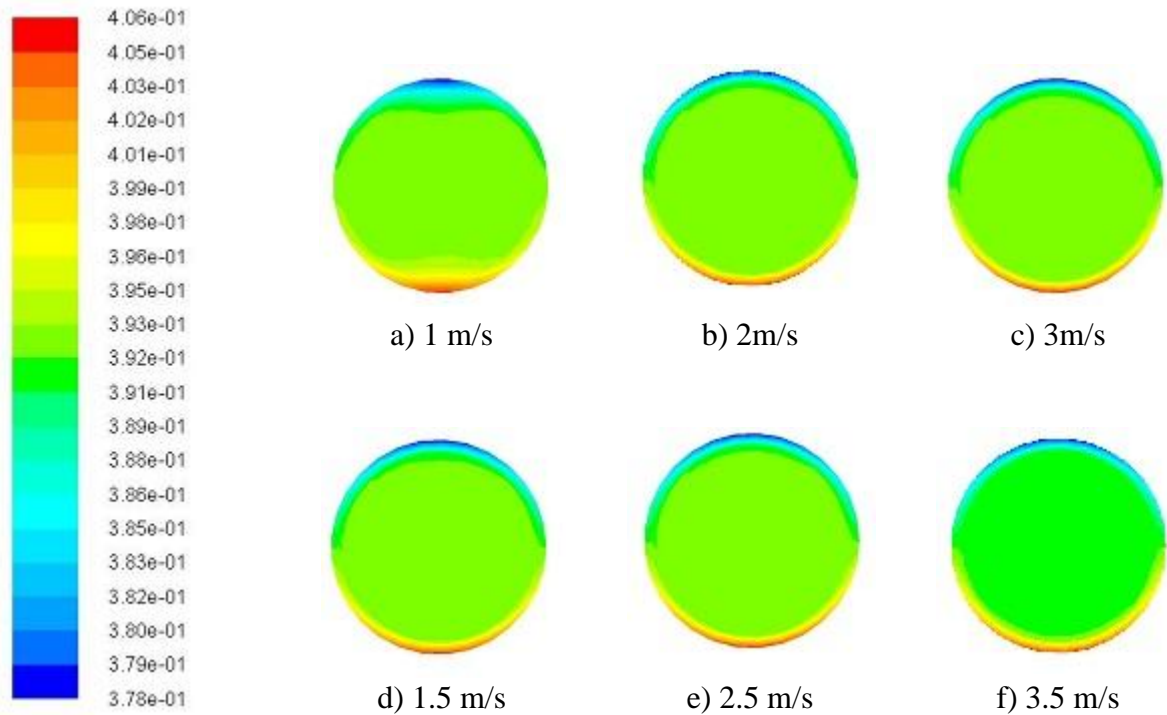


Fig 4.11 (iii) CFD predicted solid volume fraction contour at 60% concentration by weight at different velocities

It is clearly shown in the above figures that as the velocity increases the particles starts lifting up toward the center of the pipe as against at low velocities, where particles have the tendency to settle down due to gravitational force acting on them.

4.5.3 Velocity Profile

As the experimental data for the vertical velocity profile is not available, the validation of the experimental and predicted velocity profile could not be judged, but the predicted velocity profile agrees the theoretical understanding. Therefore, conclusion is made indirectly that CFD simulation is capable of validating the velocity profile. As shown in below figures that solid phase velocity profile is generally asymmetric in nature about longitudinal axis at low velocities, which is due to settling of particles because of density difference. At higher velocities this asymmetrical nature is reduced but still the most of the particles remain in lower half of the pipe.

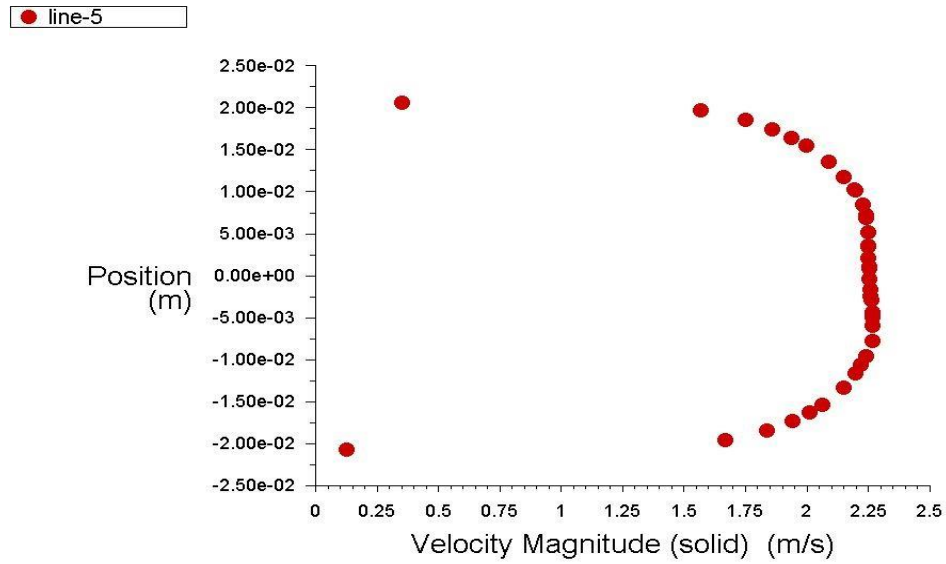


Fig. 4.14 Vertical velocity profile at 2 m/s at 60% concentration by weight

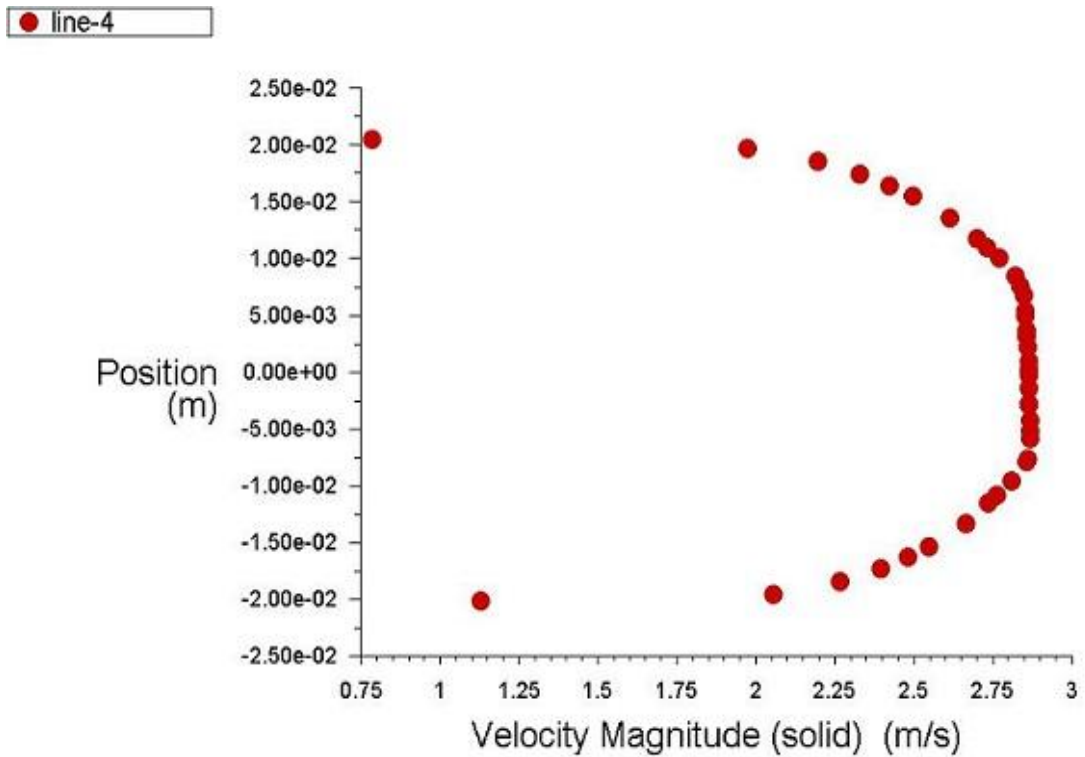


Fig. 4.15 Vertical velocity profile at 2.5 m/s at 60% concentration by weight

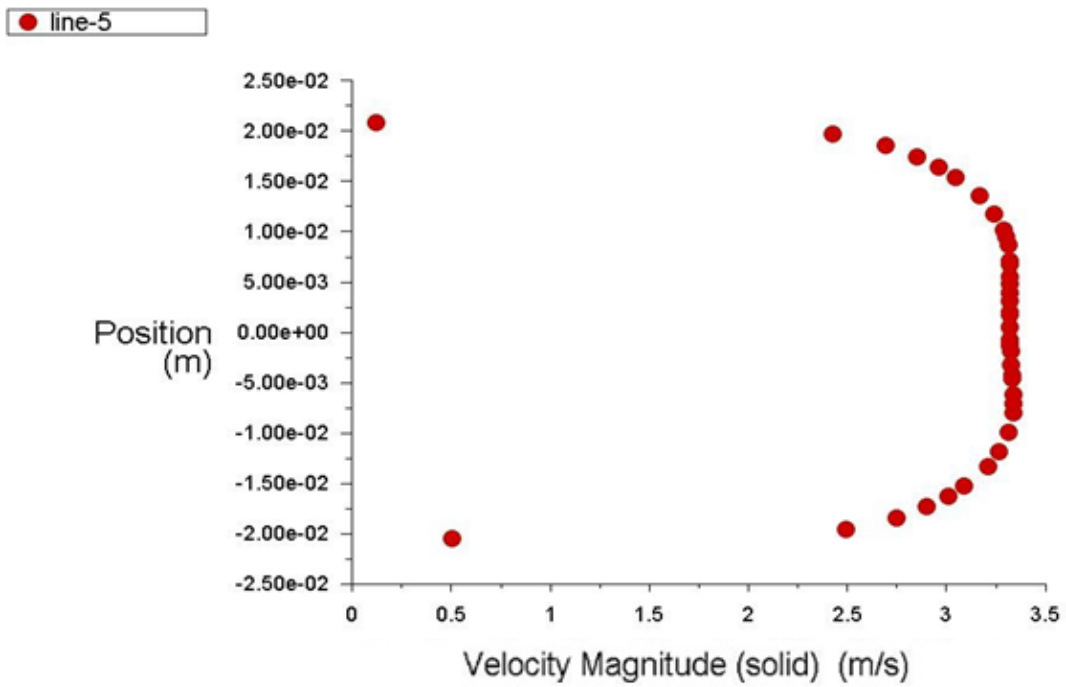


Fig. 4.16 Vertical velocity profile at 3 m/s at 60% concentration by weight

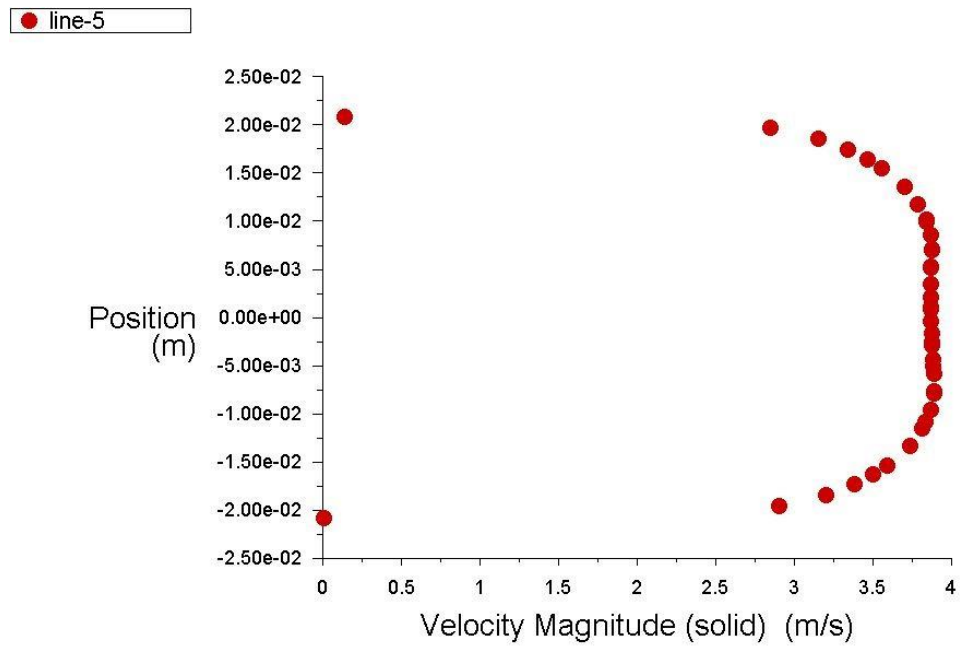


Fig. 4.17 Vertical velocity profile at 3.5 m/s at 60% concentration by weight

4.6 Effect of Particle Size

Solid particle size in above simulation for zinc slurry is about $33\ \mu\text{m}$ which make the slurry homogenous in nature in which all the particles are nearly remains suspended in carrier fluid, now the effect of increasing particle size on the pressure drop, concentration profile and velocity profile is estimated with CFD simulation. Particle size is increased from $33\ \mu\text{m}$ to $110\ \mu\text{m}$ which changes the nature of flow regime from homogenous to heterogeneous.

4.6.1 Effect of particle size on pressure drop and Power required

Pressure drop along the length of pipe is increases with increase in both velocity and concentration of the solid particles. For fine particle slurry the pressure drop increase slowly at low velocities but increase drastically at higher velocities, this is due to increase in the surface area which results in increase in friction. On the other hand for coarse particle slurry pressure drop increase is large at low velocities which are due to settling of solid particles due to gravity and formation of bed at bottom of pipe at low velocities. But at high velocities the increase in pressure drop is relatively small as compare to that at low velocities this is due to increase in turbulent energy which makes the solid particles remain suspended in carrier fluid which is shown in below fig. 4.18(a) and in fig. 4.18(b) power required is shown.

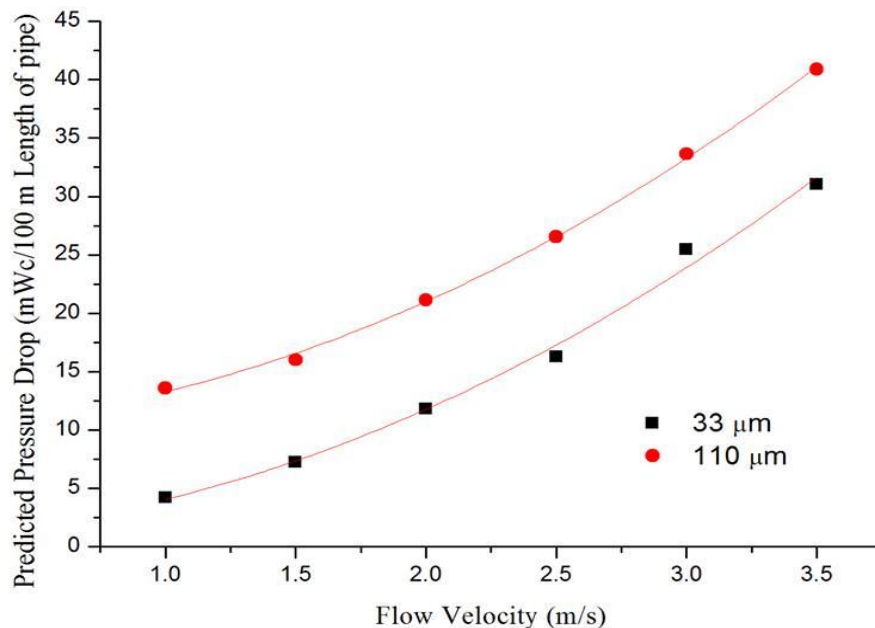


Fig. 4.18(a) Comparison of pressure drop at different velocities at 40% concentration by weight of zinc slurry at two different particle sizes.

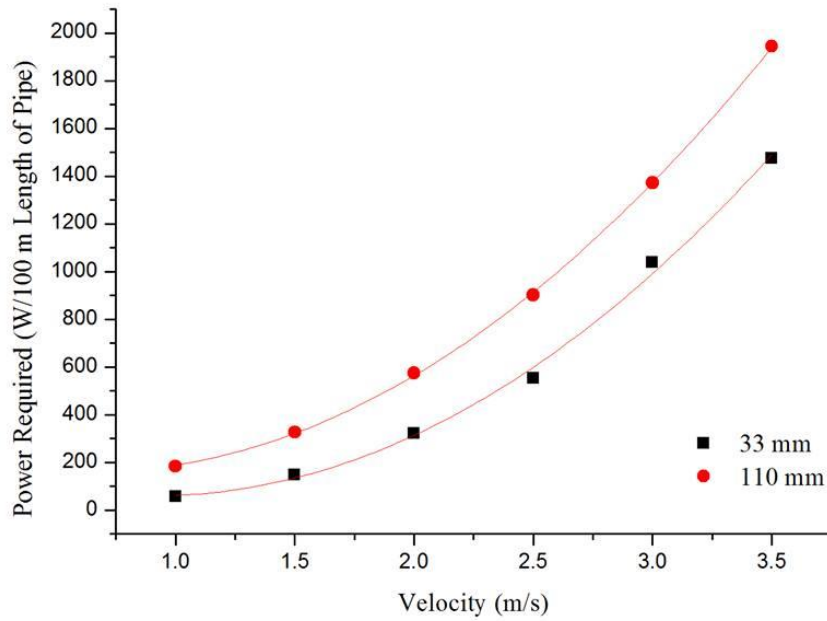
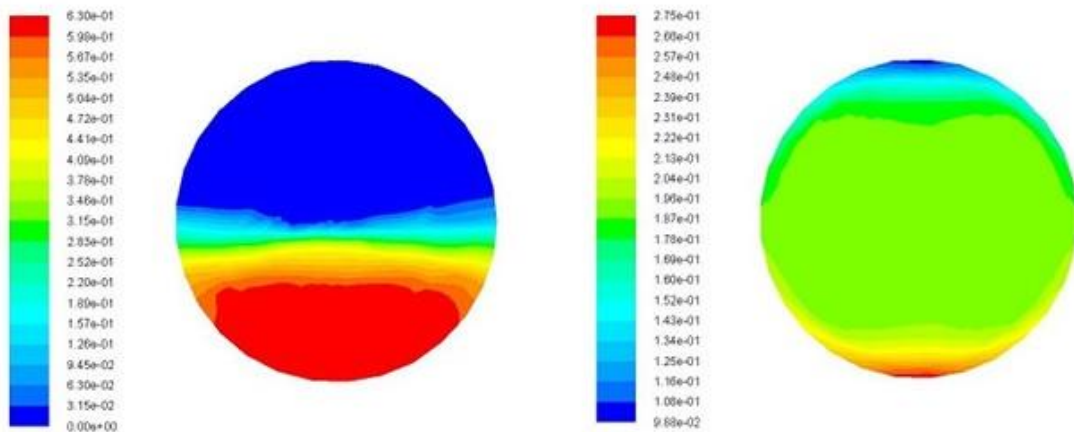


Fig.4.18(b) Power consumption at 40% concentration at different velocities for zinc slurry at two different particle sizes.

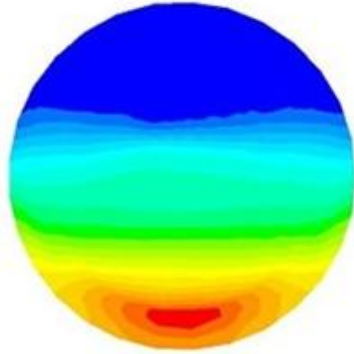
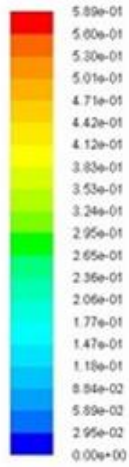
4.6.2 Effect of Particle Size on Solid Volume Fraction Contour

As discussed above that in fine particle slurry the flow regime is homogenous in which the particles remains suspended throughout the cross section of the pipe with little settling, but that is not the case with coarse particle slurry in which particles settle down due to gravity effect at lower velocities and starts lifting towards the center of pipe at higher velocities which is shown in fig. 4.19

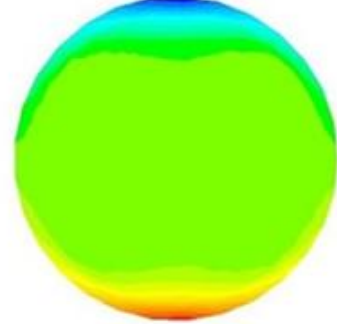
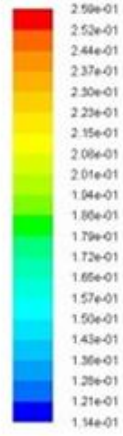


a) 110 μ m particles at 1m/s

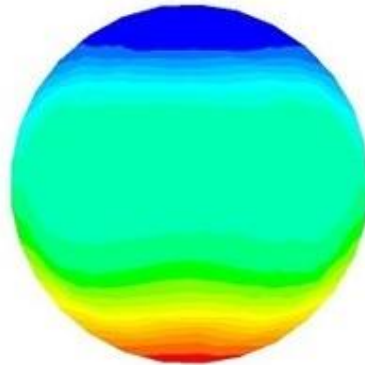
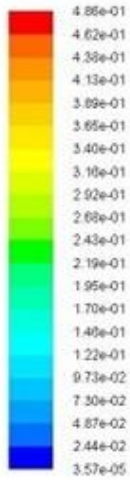
b) 33 μ m particles at 1m/s



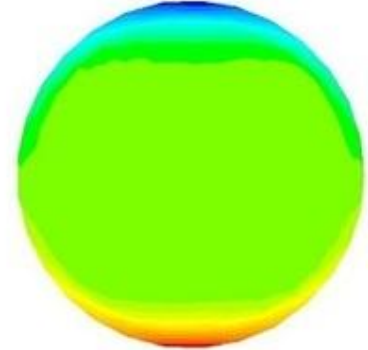
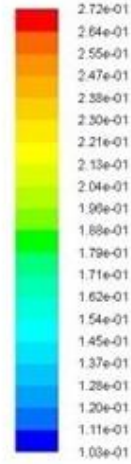
c) 110 μm particles at 2m/s



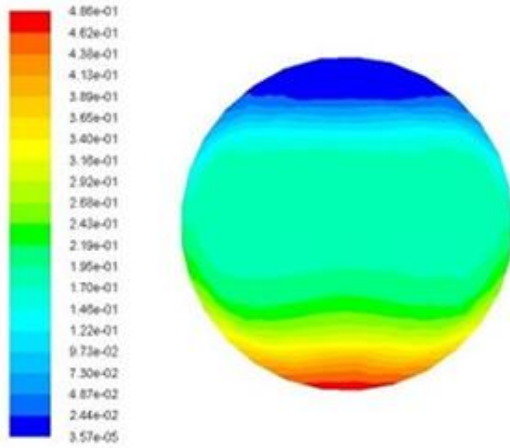
d) 33 μm particles at 2m/s



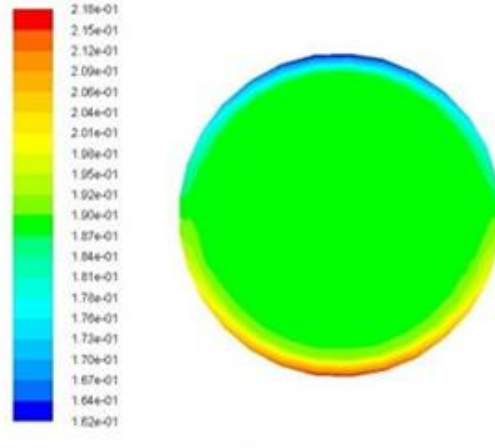
e) 110 μm particles at 2.5m/s



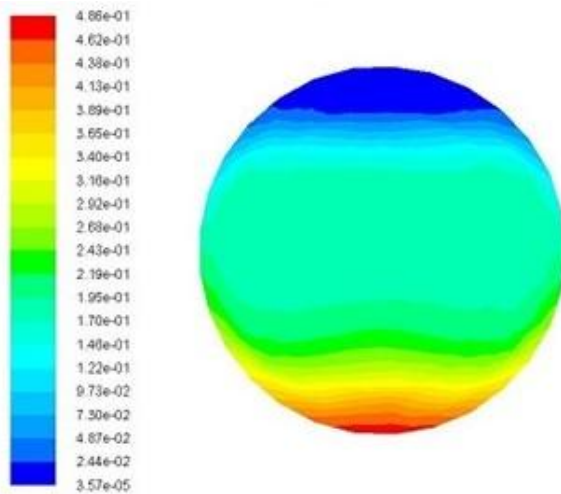
f) 33 μm particles at 2.5m/s



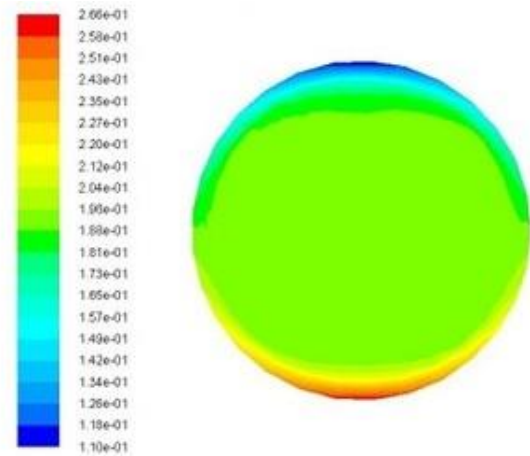
g) 110 μm particles at 3 m/s



h) 33 μm particles at 3 m/s



i) 110 μm particles at 3.5 m/s



j) 33 μm particles at 3.5 m/s

Fig.4.19 Comparison of solid volume fraction contours at different velocities at 40% concentration by weight of zinc slurry at two different particles size.

From the figures above it is observed that variation of solid concentration in horizontal plane is more noticeable as the velocity increases. For most of the data, the higher concentration zone is situated in the lower half portion at the bottom of the pipe, which is due to gravitational effect. However, with increase in velocity of flow, the higher concentration zones are situated in the lower half portion of the pipeline away from the surrounding pipe wall.

5.1 Conclusions

The capability of CFD, in this study, is explored to model complex solid liquid slurry flow in pipeline. The commercial CFD software (FLUENT) is found capable to successfully model the solid liquid interactions in slurry flow. Following conclusions have been drawn on the basis of present study.

- 1) It has been observed that at higher velocities, the higher concentration zone is situated at lower part of pipeline away from the bottom of the pipe.
- 2) With decrease in velocity slurry starts settling, higher concentration zone moves toward the bottom of the pipe, which is due to gravity effect and decrease in the turbulent energy, which makes the particles suspended in the slurry.
- 3) It is observed that the particles are asymmetrically distributed in the vertical plane with degree of asymmetry increases with increase in particle size because of gravitational effect.
- 4) A distinct change in the shape of concentration profiles was observed indicating the sliding bed regime for coarser particles at lower flow velocities.
- 5) Pressure drop at any particular velocity increase with increase in the concentration of the bottom ash. The rate of increase of pressure is small at lower velocities but it increase drastically at higher velocities.
- 6) For fine particle slurry the pressure drop increase slowly at low velocities but increase drastically at higher velocities, this is due to increase in the surface area which results in increase in friction.
- 7) For coarse particle slurry pressure drop increase is large at low velocities which are due to settling of solid particles due to gravity and formation of bed at bottom of pipe at low velocities. But at high velocities the increase in pressure drop is relatively small as compare to that at low velocities this is due to increase in turbulent energy which makes the solid particles remain suspended in carrier fluid

5.2 Future Scope

The present research work aims at prediction of pressure drop, velocity profile and concentration profile of slurry flow in straight pipeline. But as we know that slurry transport system also encounters different pipe bends (40° , 60° , 90°), converging section, diverging section etc. so this work can be augmented by doing numerical simulation on these bends and sections.

REFERENCES

- [1] Anderson, J., 1995, Computational Fluid Dynamics, Mcgraw-Hill.
- [2] Abulnaga, B., 2002, Slurry System Handbook, Mcgraw-Hill.
- [3] Skudarnov, P.V., Lin, C.X., Ebadian, M.A., 2004, Double-Species Slurry Flow in a Horizontal Pipeline, Journal of Fluid Engineering, 126, 125-132.
- [4] Brennen, C.E., 2005, Fundamentals of Multiphase Flow, Cambridge university press.
- [5] Kaushal, D.R., Sato, K., Toyota, T., Funatsu, K., Tomita, Y., 2005, Effect of Particle Size Distribution on Pressure Drop and Concentration Profile in Pipeline Flow of Highly Concentrated Slurry, International Journal of Multiphase Flow, 31, 809-823.
- [6] Wilson, K.C., Addie, G.R., Sellgren, A., Clift, R., 2005, Slurry Transport Using Centrifugal Pumps, Springer.
- [7] Verma, A.K., Singh S.N., Seshadri V., 2006, Pressure Drop for the Flow of High Concentration Solid-Liquid Mixture Across 90° Horizontal Conventional Circular Pipe Bend, Indian Journal of Engineering & Material Sciences, 13, 477-483.
- [8] Wilcox, D.C., 2006, Turbulence Modeling for CFD, DCW Industries, Inc.
- [9] Chen, L., Duan, Y., Pu, W., Zhao, C., 2009. CFD Simulation of Coal-Water Slurry Flowing in Horizontal Pipeline. Korean Journal of Chemical Engineering 26(4), 1144-1154
- [10] Eesa, M., Barigou, M., 2009, CFD Investigation of the Pipe Transport of Coarse Solids in Laminar Power Law Fluids, Chemical Engineering Science, 64, 322-333.
- [11] Ekambara, K., Sanders, R.S., Nandakumar, K., Masliyah J.H. 2009. Hydrodynamic Simulation of Horizontal Slurry Pipeline Flow Using Ansys-Cfx, Ind. Eng. Chem. Res., 48, 8159-8171.
- [12] Lahiri S.K., Ghanta K.C., 2009, Artificial Neural Network Model with Parameter Tuning Assisted by Genetic Algorithm Technique: Study of Critical Velocity of Slurry Flow in Pipeline, Asia-Pacific Journal of Chemical Engineering, 5(5), 763-777.

- [13] Lahiri, S.K., Ghanta, K.C., 2009, Development of a Hybrid Support Vector Machine and Genetic Algorithm Model for Regime Identification of Slurry Transport in Pipelines, *Asia-Pacific Journal of Chemical Engineering*, 5(6), 847-861.
- [14] Vlasak, P., Chara, Z. 2009. Conveying of Solid Particles in Newtonian and non-Newtonian Carriers, *Particulate Science and Technology: An International Journal*, 27(5), 428-443.
- [15] Yingjie, R., Song, L., Zhang, D., Gao, J., Xu, H., 2009, Effect of Solvent on the Viscosity Changes of Coal-Oil Slurry Under High Temperature-High Pressure During Heating, *Asia-Pacific Journal of Chemical Engineering*, 4(5), 744-750.
- [16] Chandel, S., Singh S.N., Seshadri, V., 2010, Transportation of High Concentration Coal Ash Slurries Through Pipelines, *International Archieve of Applied Sciences and Technology*, 1(1), 1-9.
- [17] Lahiri, S.K., Ghanta, K.C. 2010, Slurry Flow Modeling by CFD, *Chemical Industry & Chemical Engineering Quarterly*, 16(4), 295-308.
- [18] Lei, L., Usui, H., Suzuki, H. 2010, Study of Pipeline Transportation of Dense Fly Ash-water Slurry, *Coal Preparation*, 22(2) 65-80.
- [19] Lu, H., Yin, J., Yuan, Y., Wang, J. 2010. Effect of Particle Size Distribution on Flow Pattern and Pressure Drop in Pipeline Flow of Slurries, 2nd Conference on Environmental Science and Information Application Technology.
- [20] Fluent Theory guide, 2011.
- [21] Hossain, A., Naser, J., Imteaz, J.N., 2011, CFD Investigation of Particle Deposition in a Horizontal Looped Turbulent Pipe Flow, *Environ Model Assess*, Springer, 16, 359-367.
- [22] Kaushal, D.R., Tomita, Y., 2011, An Improved Method for Predicting Pressure Drop along Slurry Pipeline, *Particulate Science and Technology : An International Journal*, 20(4), 305-324.
- [23] Mazumder, Q.H., 2011, CFD Analysis of Effect of Elbow Radius on Pressure Drop in multiphase Flow, *Modelling and Simulation in Engineering*, doi:10.1155/2012/125405.

- [24] Vlasak, P., Chara, Z. 2011, Effect of particle size distribution and concentration on flow behavior of dense slurries, *Particulate Science and Technology : An International Journal*, 29(1), 53-65.
- [25] Kaushal, D.R., Thinglas, T., Tomita, Y., Kuchii, S., Tsukamoto, H. 2012. CFD Modeling for Pipeline Flow of Fine Particles at High Concentration. *International Journal of Multiphase Flow* 43, 85-100.
- [26] Xiuyuan, M., Duan, Y., Liu. M., Li, H., 2012, Influence of Sewage Sludge on the Rheological Properties of Petroleum Coke-Water Slurry, *Asia-Pacific Journal of Chemical Engineering*, 8(3), 453-460.
- [27] Kumar, N., Kaushal, D.R., Kumar, A., 2012, Computational Study of the Two Phase Flow in Horizontal Slurry Pipeline, *International Journal of Mechanical and Production Engineering (IJMPE)* , 1(1), 2315-4489.
- [28] Mazumder, Q.H., 2012, CFD Analysis of the Effect of Elbow Radius on Pressure Drop in Multiphase Flow, *Modelling and Simulation in Engineering*, doi:10.1155/2012/125405.
- [29] Bandhyopadhyay, T.K., Das, S.K., 2013, Non-Newtonian and Gas-non-Newtonian Liquid Flow through Elbows –CFD Analysis, *Journal of Applied Fluid Mechanics*, 6(1), 131-141.
- [30] Capecelatro J., Desjardins O, 2013. Eulerian-Lagrangian Modeling of Turbulent Liquid-Solid Slurries in Horizontal Pipes, *International Journal of Multiphase Flow*, 55, 64-79.
- [31] Kaushal, D.R., Kumar, A., Tomita, Y., Kuchii, S., Tsukamoto, H., 2013, Flow of Mono-Dispersed Particles Through Horizontal Bend, *International Journal of Multiphase Flow*, 52, 71-91.
- [32] Kaushal, D.R., Kumar, N., 2013, Optimum Design of High Concentration Fly Ash Slurry Disposal Pipeline, *Electronic Journal of Polish Agricultural Universities*, 6(4).
- [33] Nabil, T., Sawaf, El I., Nahhas El K., 2013, Computational Fluid Dynamics Simulation of the Solid Liquid Slurry Flow in a Pipeline, *Seventh International Water Technology Conference, IWTC 17, Istanbul*.